

# An Attempt to Programme the Orientation of Bis(heterocyclic) Azine Heterotopic Sequences around $\text{Ag}^{\text{I}}$ , $\text{Cu}^{\text{I}}$ and $\text{Zn}^{\text{II}}$ Metal Centres

Julien Mathieu,<sup>[b]</sup> Nouredine Ghermani,<sup>[a]</sup> Nouzha Bouhaida,<sup>[c]</sup> Bernard Fenet,<sup>[d]</sup> and Alain Marsura\*<sup>[b]</sup>

**Keywords:** Self-assembly / Self-recognition / Heterocyclic bidentate sequences /  $\text{Cu}^{\text{I}}$ ,  $\text{Ag}^{\text{I}}$ ,  $\text{Zn}^{\text{II}}$  metal complexes

Four novel bis(heterocyclic) sequences, which incorporate a 2,2'-bipyridine system with the 2,2'-bithiazole, 4,4'-bithiazole, 2,2'-bipyrazine or 4,4'-bipyrimidine units, have been synthesized. In the presence of stoichiometric amounts of  $\text{Cu}^{\text{I}}$ ,  $\text{Ag}^{\text{I}}$  or  $\text{Zn}^{\text{II}}$  cations, fully oriented discrete head-to-head (H-H) or head-to-tail (H-T) species have been observed by NMR and X-ray crystallography. The orientation of the li-

gands in the  $\text{Ag}^{\text{I}}$ ,  $\text{Cu}^{\text{I}}$  or  $\text{Zn}^{\text{II}}$  dinuclear complexes during the self-assembly process appears to be under the control of electronic factors relating to the electronic configuration of the different bis(heterocyclic) sequences.

(© Wiley-VCH Verlag GmbH & Co. KGaA, 69451 Weinheim, Germany, 2004)

## Introduction

The design and study of double- and triple-stranded helical complexes obtained by self-assembly of two or three ligand strands with metal ions has been the subject of several recent detailed investigations and literature reviews.<sup>[1,2]</sup> Architectural information is expressed in the matching between the ligand binding sites and the stereochemical preferences of the metal ion.

Of the numerous helical structures already published, the spontaneous formation of double-stranded homodimetallic<sup>[2a–2c]</sup> or heterodimetallic<sup>[2f–2i]</sup> helicates has been studied extensively. The formation of helicates depends on the nature of the metal ions and ligands and sometimes on additional factors introduced by appropriate

templating.<sup>[3]</sup> Some years ago, a first event was observed in the case of  $\text{Ga}^{\text{III}}$  and  $\text{Ti}^{\text{V}}$  aminophenolate/catecholate complexes where the phenolic protons were abstracted allowing the formation of the corresponding dinuclear oriented triple-stranded helicates.<sup>[4]</sup> The selectivity of these assemblies in discriminating between a nitrogen (amine) and an oxygen (hydroxy) atom of a biphenylene structure was obviously influenced by the difference of reactivity between the two coordinating centres.

Recently, we described another kind of strongly induced selectivity in the case of a  $\text{Cu}^{\text{I}}$  double-stranded head-to-tail (H-T) spontaneous assembly obtained from a bipyridine-bipyrazine sequence.<sup>[5]</sup> In that case, the final complex was formed solely by the coordination of  $\text{Cu}^{\text{I}}$  to the imino nitrogen lone pairs of the heterocycles without the need for external hindered factors or other stereochemical requirements. Additionally, we have reported ab initio theoretical calculations dealing with the probable origin of the observed selectivity.<sup>[6]</sup> According to the stereochemistry found in the helicate, an electron back-donating effect was found to be responsible for the better stability of the heterotopic complexes (bipyridine–Cu–bipyrazine) compared to the homotopic ones.<sup>[6]</sup> This feature clearly suggests that the aromatic nature of the heterocycles themselves could play a decisive role on orientation within the final helicate.

In order to verify the generality of this assumption for other ligands, we have prepared four novel bis(heterocyclic) heterotopic saturated sequences, which incorporate a 2,2'-bipyridine nucleus together with a 2,2'-bithiazole, 4,4'-bithiazole, 2,2'-bipyrazine or 4,4'-bipyrimidine bis(heterocyclic) unit. The formation of the corresponding  $\text{Ag}^{\text{I}}$ ,  $\text{Zn}^{\text{II}}$

<sup>[a]</sup> Laboratoire de Physique Pharmaceutique UMR 8612, Université Paris XI, Faculté de Pharmacie, 5 rue J. B. Clément, 92296 Châtenay-Malabry, France  
Fax: (internat.) + 33-1-46835882  
E-mail: noureddine.ghermani@cep.u-psud.fr

<sup>[b]</sup> GEVSM Unité Mixte de Recherche du CNRS, Structure et Réactivité des Systèmes Moléculaires Complexes, 5 rue A. Lebrun, B. P. 403, 54001 Nancy Cedex, France  
Fax: (internat.) + 33-3-83682345  
E-mail: Alain.Marsura@pharma.uhp-nancy.fr

<sup>[c]</sup> Laboratoire des Sciences des Matériaux, LSM, Université Cadi Ayyad, Faculté des Sciences Semlalia, Boulevard Prince Moulay Abdallah, B. P. 2390, 40000 Marrakech, Morocco  
E-mail: nouzha@ucam.ac.ma

<sup>[d]</sup> Centre de RMN Université Claude Bernard, Lyon-1/ESCPE, Domaine Scientifique de la Doua, Boulevard du 11 Novembre 1918, 69100 Villeurbanne Cedex, France  
E-mail: bernard.fenet@univ-lyon1.fr

Supporting information for this article is available on the WWW under <http://www.eurjic.org> or from the author.

and Cu<sup>I</sup> complexes with these ligands and the X-ray structure analysis of the Cu<sup>I</sup> and Ag<sup>I</sup> dinuclear helicates revealed a fully selective H-T and H-H orientation of the strands within the helicates.

## Results and Discussion

### Synthesis of Ligands 9 to 12

In order to explore the scope and limitations of a possible programming of oriented double-stranded helicates from discrete bis(heterocyclic) azines, we prepared the new li-

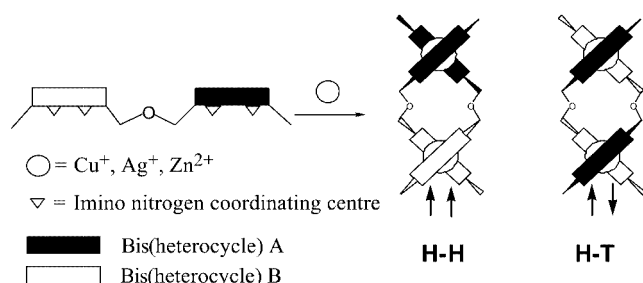
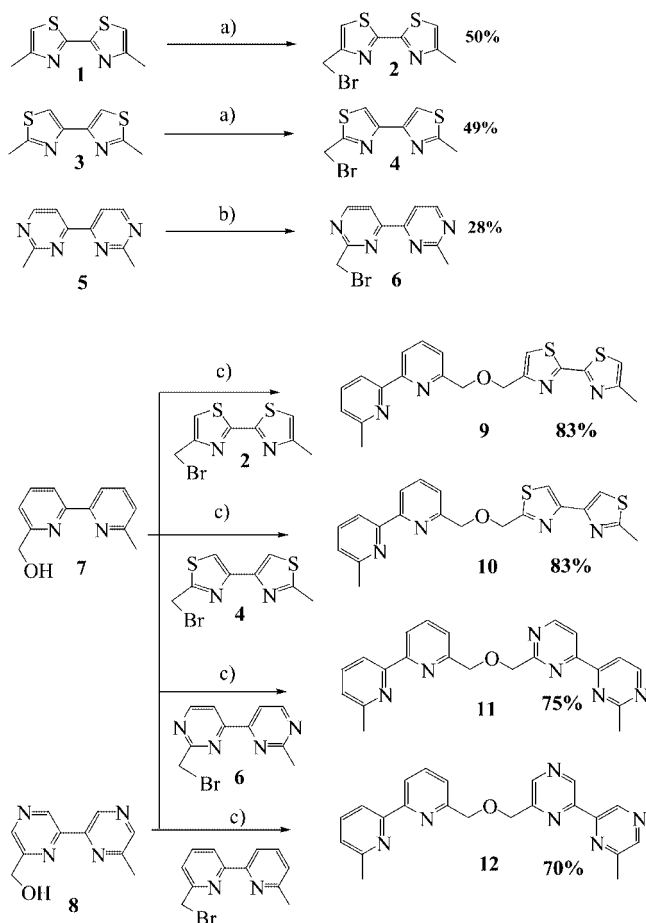


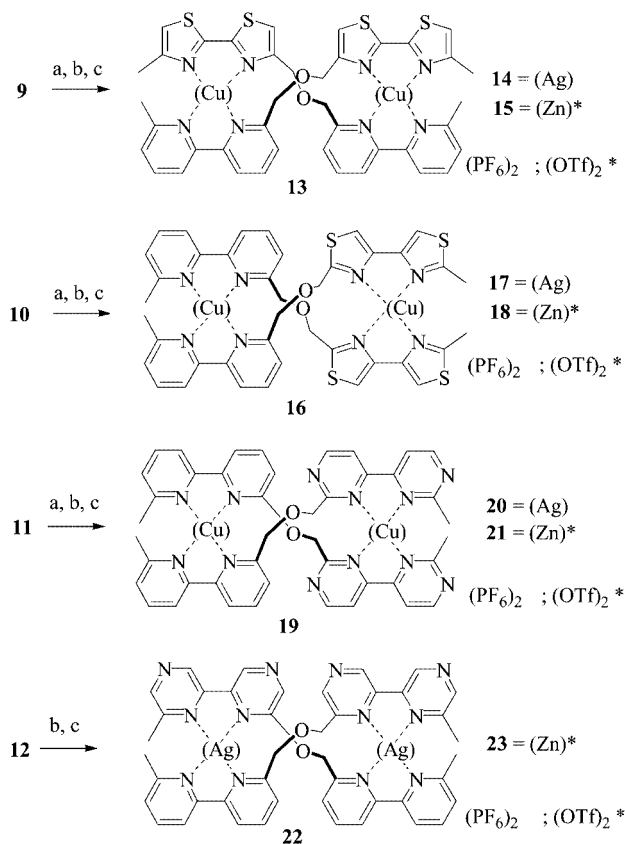
Figure 1. Graphical illustration of the self-assembly strategy



Scheme 1. Synthesis of 7 and 8: a) NBS, benzoyl peroxide, CCl<sub>4</sub>, reflux, hv; b) NBS, AIBN, reflux, hv; c) NaH, THF under Ar, 0 °C

gands 9–12 containing a 2,2'-bithiazole, a 4,4'-bithiazole, a 2,2'-bipyrazine or a 4,4'-bipyrimidine unit, respectively, together with a common 2,2'-bipyridine nucleus. These ligands were designed in order that the non-identical bis(heterocyclic) components present two identical bis(diimine) coordinating centres connected by an oxopropylene bridge. Therefore, in the presence of geometrically tetrahedral coordinating cations, there are two possible orientations for the ligands around the metal atom in a dinuclear complex: H-H (head-to-head) or H-T (head-to-tail) (Figure 1).

Ligand 9 (Scheme 1) was prepared from the dimethyl-2,2'-bithiazole 1,<sup>[7]</sup> ligand 10 from the dimethyl-4,4'-bithiazole 3,<sup>[8]</sup> ligand 11 from 2,2'-dimethyl-4,4'-bipyrimidine (5)<sup>[9]</sup> and ligand 12 from 6,6'-dimethyl-2,2'-bipyrazine by a previously reported method.<sup>[5]</sup> The bis(heterocycles) were transformed into 6-(monobromomethyl) 2, 4 and 6 derivatives or 6-(monohydroxymethyl) derivatives 7 and 8, respectively. The final ligands were obtained in good yields (70–83%) after Williamson condensation of the (monobromomethyl)bithiazoles, -bipyrimidine or -bipyridine with 6-(hydroxymethyl)-6'-methyl-2,2'-bipyridine<sup>[10]</sup> or 6-(hydroxymethyl)-6'-methyl-2,2'-bipyrazine,<sup>[5]</sup> respectively. Addition of previously prepared [Cu(CH<sub>3</sub>CN)<sub>4</sub>]PF<sub>6</sub> or commercially available Ag(PF<sub>6</sub>) to solutions of 9–12 in anhydrous acetonitrile or addition of Zn(OTf)<sub>2</sub> to solutions of the ligands in MeOH affords the corresponding copper, silver or zinc dinuclear complexes (Scheme 2). Addition of the



Scheme 2. Synthesis of complexes 13–23: a) [Cu(CH<sub>3</sub>CN)<sub>4</sub>]PF<sub>6</sub>; b) AgPF<sub>6</sub>; c) Zn(OTf)<sub>2</sub>; (OTf = triflate anion)

metal ion solutions resulted in instant colour changes from colourless to deep-red or deep-orange in the case of  $\text{Cu}^{\text{I}}$  or colourless to pale yellow in the case of the  $\text{Ag}^{\text{I}}$  and  $\text{Zn}^{\text{II}}$  indicating the effective formation of the complexes. A thin layer chromatographic control showed that the free ligand was totally consumed in the reaction. The crude materials were recrystallized by slow diffusion of diethyl ether into acetonitrile or acetone solutions (copper and silver complexes) or by slow concentration of a methanolic solution in the case of zinc complexes (see Exp. Sect.). The deep red crystals with  $\text{Cu}^{\text{I}}$  and the pale yellow crystals with  $\text{Ag}^{\text{I}}$  and  $\text{Zn}^{\text{II}}$  are stable in air. In each case, the ligands form the expected dinuclear double-stranded helical structures as observed by X-ray diffraction analyses.

### Thermodynamic Self-Assembly Processes of Ligands 9–12 with $\text{Cu}^{\text{I}}$ , $\text{Ag}^{\text{I}}$ and $\text{Zn}^{\text{II}}$

The formation of the double-helical metal complexes 13–23 was followed by UV/Vis spectrophotometric titration of ligands 9–12 with  $\text{Cu}[\text{CH}_3\text{CN}]_4[\text{PF}_6]_2$ ,  $\text{AgPF}_6$  in  $\text{CH}_3\text{CN}$  or  $\text{Zn}(\text{OTf})_2$  in MeOH. Titrations of ligand 9 with  $\text{Cu}[\text{CH}_3\text{CN}]_4[\text{PF}_6]_2$  (Figure 2) and ligand 11 with  $\text{Zn}(\text{OTf})_2$  (Figure 3) are presented as typical examples (see Supporting Information for other titration data; see the footnote on the first page of this article). Spectra obtained during titration of ligand 9 display two sharp isobestic points between 250 and 600 nm over the duration of the titration. The colourless solution of 9 becomes red instantly upon addition of  $\text{Cu}[\text{CH}_3\text{CN}]_4[\text{PF}_6]_2$  owing to the appearance of an MLCT band at  $\lambda_{\text{max.}} = 450 \text{ nm}$  ( $\epsilon = 1700$ ) and indicating coordination of the  $\text{Cu}^{\text{I}}$  atoms. The titration plot (see B in Figure 2) indicates that the species formed has a composition of ca. 1 Cu atom for 1 equiv. of 9 in agreement with the stoichiometry expected for the double-stranded helicate  $[\text{Cu}_2(\mathbf{9})_2][\text{PF}_6]_2$  (13). Conversely, the titration spectra of ligand 11 display, on addition of  $\text{Zn}(\text{OTf})_2$ , the successive appearance of two strong and distinct absorptions at  $\lambda_{\text{max.}} = 304 \text{ nm}$  ( $\epsilon = 17650$ ) and  $\lambda_{\text{max.}} = 316 \text{ nm}$  ( $\epsilon = 18970$ ) indicating the effective coordination of the  $\text{Zn}^{\text{II}}$  atoms. The titration plot (B in Figure 3) reveals that the

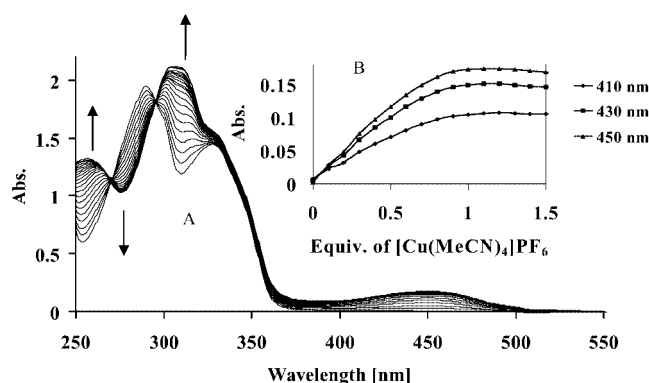


Figure 2. Spectrophotometric titration of ligand 9 with  $[\text{Cu}(\text{MeCN})_4]\text{PF}_6$  (0.1–1.5 equiv.) in acetonitrile: A) UV/Vis absorption spectra and B) Plots of absorbance versus added salt equiv. at three wavelengths

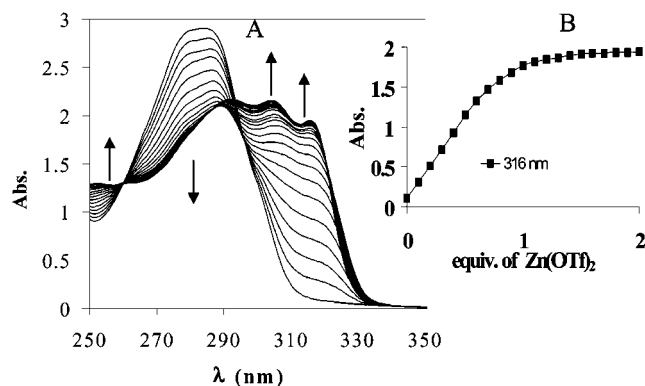


Figure 3. Spectrophotometric titration of ligand 11 with  $\text{Zn}(\text{OTf})_2$  (0.1–2.0 equiv.) in MeOH: A) UV/Vis absorption spectra and B) plot of absorbance versus added salt equiv. at 316 nm

species formed has a composition of ca. 1 Zn atom for 1 equiv. of 11 in agreement with the expected stoichiometry of 21. A similar difference is observed in the formation of complex 18 containing  $\text{Zn}^{\text{II}}$  but not with the formation of the other zinc complexes or the other metal complexes investigated. This suggests that the two zinc ions were complexed in a different environment in the other species.

Analysis of titration data provides the thermodynamic parameters of dihelicate formation. Factor analysis points to the existence of five absorbing species ( $L$ ,  $ML$ ,  $M_2L$ ,  $ML_2$ ,  $M_2L_2$ ) and the spectrophotometric data can be fitted to the equilibria given below [Equations (1) and (2)], which characterize the assembly process and are described by stability constants ( $\beta_{mi}$ ). Using the SPECFIT program,<sup>[11]</sup> the binding constants  $\log(\beta_{mi})$  for each species  $M_mL_l$  have been calculated (Table 1).



The species  $M_2L$  and  $ML_2$  were neglected because they

Table 1. Formation constants  $\log(\beta_{mi})$  for the complexes  $[\text{M}_2\text{L}_2]^{n+}$  (13–23) in acetonitrile and methanol (\*) at 298 K<sup>[11]</sup>

$[\text{M}_2(\text{L})_2]^{n+}$	$\log \beta_{11}$	$\log \beta_{22}$
$[\text{Cu}_2(\mathbf{9})_2]^{2+}$ (13)	$5.9 \pm 0.1$	$23.7 \pm 2.0$
$[\text{Ag}_2(\mathbf{9})_2]^{2+}$ (14)	$5.1 \pm 0.1$	$22.5 \pm 1.7$
$[\text{Zn}_2(\mathbf{9})_2]^{4+}$ (15)*	$6.2 \pm 0.3$	$23.3 \pm 1.9$
$[\text{Cu}_2(\mathbf{10})_2]^{2+}$ (16)	$3.9 \pm 0.2$	$16.4 \pm 1.5$
$[\text{Ag}_2(\mathbf{10})_2]^{2+}$ (17)	$5.3 \pm 0.1$	$23.4 \pm 1.8$
$[\text{Zn}_2(\mathbf{10})_2]^{4+}$ (18)*	$4.9 \pm 0.1$	$21.4 \pm 1.4$
$[\text{Cu}_2(\mathbf{11})_2]^{2+}$ (19)	$4.3 \pm 0.1$	$19.1 \pm 1.9$
$[\text{Ag}_2(\mathbf{11})_2]^{2+}$ (20)	$4.8 \pm 0.1$	$21.3 \pm 1.4$
$[\text{Zn}_2(\mathbf{11})_2]^{4+}$ (21)*	$5.9 \pm 0.2$	$19.3 \pm 0.2$
$[\text{Cu}_2(\mathbf{12})_2]^{2+}$ [5]	$5.6 \pm 0.1$	$19.6 \pm 1.8$
$[\text{Ag}_2(\mathbf{12})_2]^{2+}$ (22)	$5.3 \pm 0.4$	$23.3 \pm 1.9$
$[\text{Zn}_2(\mathbf{12})_2]^{4+}$ (23)*	$5.2 \pm 0.1$	$23.6 \pm 1.9$

were present only in negligible quantities under the experimental conditions used here.

Positive-mode ESI-MS spectra of all the complexes contained doubly charged ions except for the Zn<sup>II</sup> complexes in which quadruply charged ions were detected. For illustration, mass spectra of the copper and zinc complexes **13** and **15** (Figure 4) reveal the [Cu<sub>2</sub>(**9**)<sub>2</sub>]<sup>2+</sup> doubly charged ion (*m/z* = 457 a.m.u.) (peak separated by 0.5 a.m.u.) and the [Cu<sub>2</sub>(**9**)<sub>2</sub>(PF<sub>6</sub>)<sub>2</sub>]<sup>+</sup> singly charged ion (*m/z* = 1059 a.m.u.), while for the zinc complex the [Zn<sub>2</sub>(**9**)<sub>2</sub>]<sup>4+</sup> quadruply charged ion (*m/z* = 229 a.m.u.) (peak separated by 0.25 a.m.u.) and the [Zn<sub>2</sub>(**9**)<sub>2</sub>(OTf)<sub>3</sub>]<sup>+</sup> singly charged ion (*m/z* = 1364 a.m.u.) are observed. These results are only compatible with the formation of double-stranded helicates.<sup>[12]</sup> Similar results were obtained with the other complexes.<sup>[13]</sup>

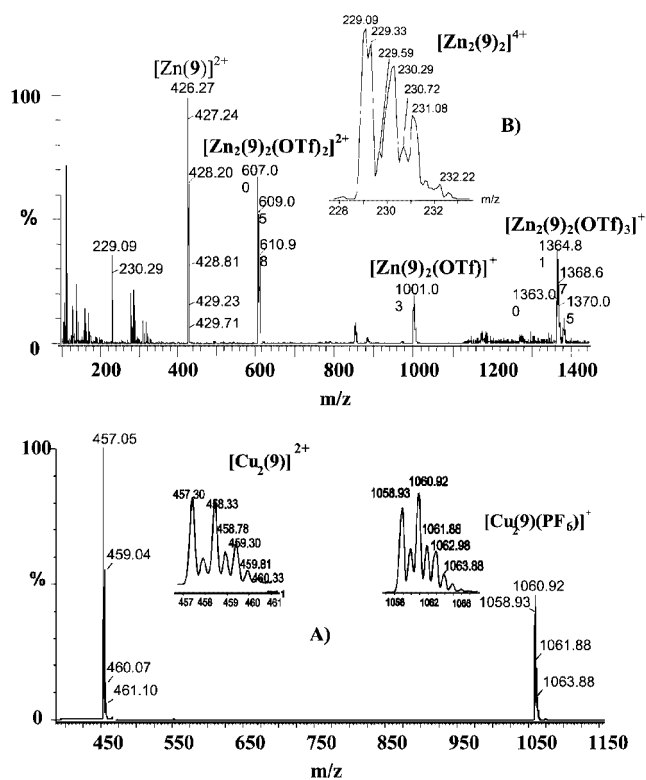


Figure 4. Positive-ion ESI mass spectra of complexes: A) **13** and B) **15**

### NMR Analysis

The <sup>1</sup>H NMR spectra of the free ligands **9**–**12** give resolved first-order spectra and each proton of each bis(heterocycle) in the ligand was assigned on the basis of COSY-LR NMR experiments. Complexation of metal ions by the ligand causes upfield or downfield shifts of all the ligand proton <sup>1</sup>H NMR signals indicating the effective formation of the complexes (see for example Figure 5).

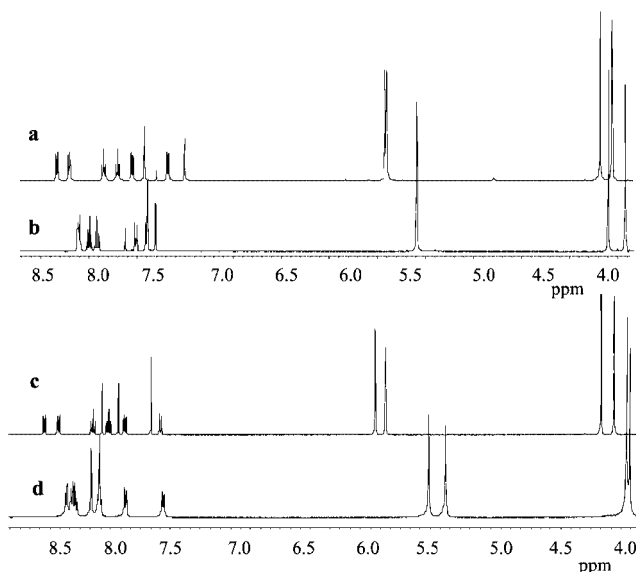


Figure 5. <sup>1</sup>H NMR spectra (400 MHz, 298 K, CDCl<sub>3</sub>/CD<sub>3</sub>CN) of a) ligand **9**; b) [Ag<sub>2</sub>(**9**)<sub>2</sub>][PF<sub>6</sub>]<sub>2</sub> (**14**); c) ligand **10**; d) [Ag<sub>2</sub>(**10**)<sub>2</sub>][PF<sub>6</sub>]<sub>2</sub> (**17**)

Significant shifts of the signals in the <sup>1</sup>H and <sup>13</sup>C NMR spectra were observed. Identical spectra were observed from in situ prepared solutions of the complexes by addition of stoichiometric amounts of the metal compound to the free ligand or from redissolution of crystals of the corresponding crystallized metal complex. At room temperature, sharp signals were observed in spectra of the silver and zinc complexes indicating the effective formation of discrete species rather than oligomeric structures. The spectra of the silver complexes **14** and **17** (Figure 5) and **20** and **22** (not shown) obtained from the 2,2'-bithiazolyl and 4,4'-bithiazolyl ligands **9**, **10** and from bipyrimidine and bipyrazine ligands **11**, **12**, respectively, show that only one species is present in solution at room temperature. The methylene protons of the oxopropylene bridges display two A<sub>2</sub> patterns (Figure 5) in place of two AB patterns, which should normally be observed for diastereotopic methylene protons in a chiral heterotopic double-helical structure.<sup>[14]</sup> This is almost certainly because of a rapid exchange under these experimental conditions as has been reported already for silver helicates.<sup>[15]</sup> <sup>1</sup>H NMR spectra of the complexes in CD<sub>3</sub>CN remain unchanged during a decrease in temperature from 333 to 233 K, and only a negligible broadening of all the signals of the whole spectrum was observed at the lowest temperature with no splitting of the methylene proton resonance into an AB pattern. In the absence of the corresponding X-ray structures for the two (bithiazolyl)silver complexes, no conclusions can be drawn from the above NMR results regarding the conformational preference of these complexes (H-H or H-T). However, variable-temperature results obtained from solutions were compatible with a side-by-side nonhelical achiral structure for these two complexes in solution although a fast exchange between chiral structures cannot be excluded because we did not observe any true line broadening in these experiments. The X-ray structures of

the silver complexes with bipyrimidyl (**20**) and bipyrazyl (**22**) ligands (see Figures 15 and 16) better corroborated the hypothesis of the existence of a chiral structure undergoing a fast exchange since they reveal that the structures of  $[\text{Ag}_2(\mathbf{11})_2]^{2+}$  (**20**) and  $[\text{Ag}_2(\mathbf{12})_2]^{2+}$  (**22**) contain double-stranded helical cations. In each case, only one species is present in the crystals having exclusively an H-H or an H-T conformation, respectively.

As previously observed for the  $[\text{Cu}_2(\mathbf{12})_2][\text{PF}_6]_2$  complex,<sup>[5]</sup> the NMR signals for compounds  $[\text{Cu}_2(\mathbf{9})_2][\text{PF}_6]_2$  (**13**),  $[\text{Cu}_2(\mathbf{10})_2][\text{PF}_6]_2$  (**16**) and  $[\text{Cu}_2(\mathbf{11})_2][\text{PF}_6]_2$  (**19**) in acetonitrile are broad and poorly resolved at room temperature<sup>[16]</sup> and display line shapes typical of exchange at moderate rate on the NMR time scale (Figure 6a). Gradually lowering the temperature of the solutions to 233 K gives resolved spectra (Figures b and 7a,b) but which are not identical with the two typical perfect AB patterns previously observed for the  $[\text{Cu}_2(\mathbf{12})_2][\text{PF}_6]_2$  double-stranded helical complex.<sup>[5]</sup> The spectra observed here display doubling of all signals indicating the presence of two species in solution at 233 K as revealed by the four different signals of methyl protons, AB and  $A_2$  patterns of oxopropylene bridge methylene protons and supplementary signals in the aromatic part of the spectrum (Figures 6b and 7a,b). Increasing the temperature results in the coalescence of the AB spin systems of the methylene protons into two  $A_2$  spin systems. This strongly indicates a loss of chirality during the exchange mechanism<sup>[16]</sup> so that only one achiral species composes the cations **16** and **19** at 353 K (see Figure 7a,b). Alternatively, there is a fast exchange between chiral structures, as proposed above in the case of the silver complexes.

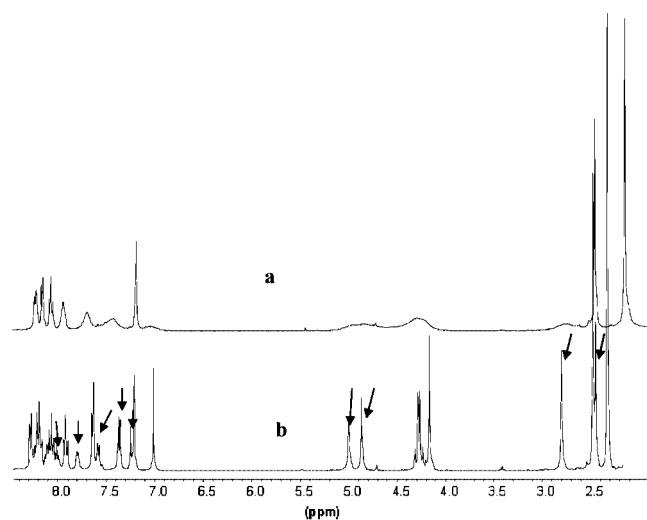


Figure 6.  $^1\text{H}$  NMR spectra (400 MHz,  $\text{CD}_3\text{CN}$ ) of  $[\text{Cu}_2(\mathbf{9})_2][\text{PF}_6]_2$  (**13**); a) 298 K, b) 233 K (arrows indicate the second species)

A deeper analysis of  $^1\text{H}$  NMR data of the  $\text{Cu}^{\text{I}}$  complexes suggested a dynamic interconversion exchange of enantiomeric helicates should occur at room temperature [dinuclear right-handed (*P*) to dinuclear left-handed (*M*)] on the NMR timescale (unresolved, large methylene proton signals) as observed for the  $[\text{Cu}_2(\mathbf{12})_2][\text{PF}_6]_2$  complex.<sup>[5]</sup> This

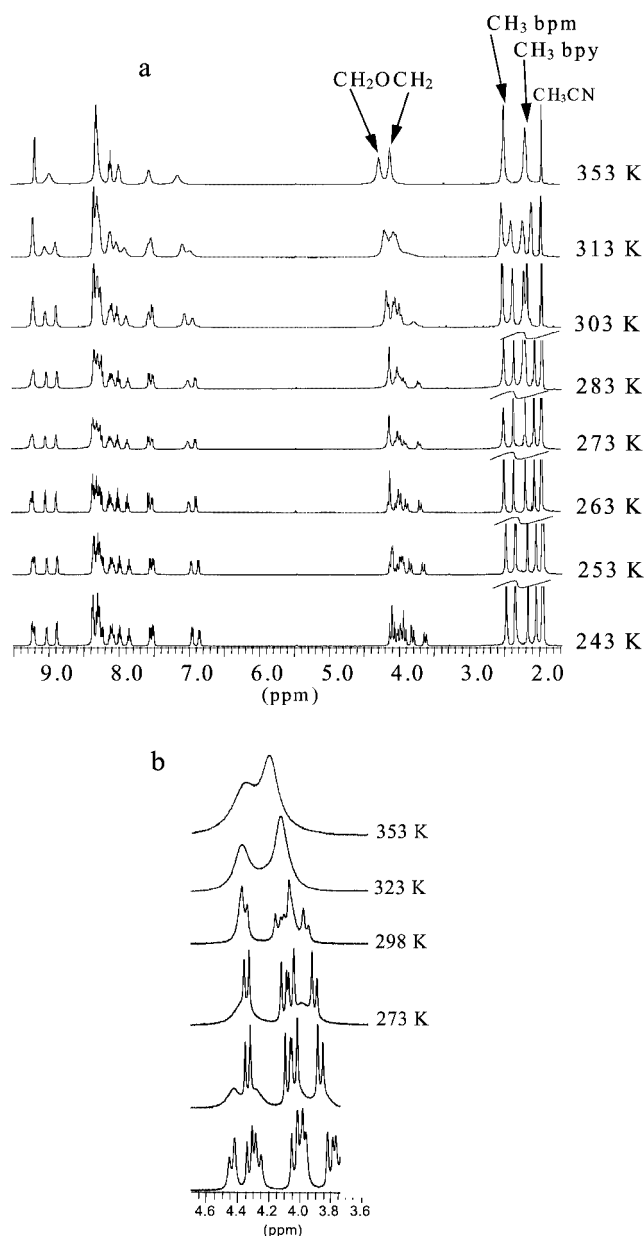


Figure 7. Variable-temperature  $^1\text{H}$  NMR spectra of a)  $[\text{Cu}_2(\mathbf{11})_2][\text{PF}_6]_2$  (**19**) (full spectra); b)  $[\text{Cu}_2(\mathbf{10})_2][\text{PF}_6]_2$  (**16**) (selected region of oxapropylene bridges) between 353 and 233 K

was confirmed by recording spectra at different temperatures (down to 233 K) revealing a sharpening of signals and a shifting and characteristic splitting of the signal of the diastereotopic methylene protons of the oxopropylene bridges. Unfortunately, this phenomenon is concomitant with the appearance of supplementary signals (methyl, oxomethylene and aromatic) which correspond to the appearance of a second species in solution. At this stage, two explanations may be advanced.

The first case entails the presence of a mixture of helical and side-by-side double-stranded dinuclear copper complexes, while the second case has a mixture of H-H and H-T conformers undergoing a rapid exchange. It should be kept in mind that the second situation can exist only by a

total and rapid decomplexation of the components, which allows inversion of the strand orientation. Additionally, it should be mentioned that, for the first hypothesis, a side-by-side complex would be observed in solution during the (*P*) ⇌ (*M*) interconversion process upon depression of the temperature. This might be considered as an intermediate conformer in the exchange mechanism between the two enantiomeric (*P*) and (*M*) helicates. In such a situation, a rapid decomplexation-recomplexation of only one helicate extremity would be sufficient. The first proposal is supported by Harding<sup>[17]</sup> and later by Greenwald<sup>[18]</sup> who made similar observations. Despite this, <sup>63</sup>Cu NMR spectra of the [Cu<sub>2</sub>(9)<sub>2</sub>][PF<sub>6</sub>]<sub>2</sub> (**13**), [Cu<sub>2</sub>(10)<sub>2</sub>][PF<sub>6</sub>]<sub>2</sub> (**16**) and the homotopic Cu<sup>I</sup> complex were investigated in order to confirm one of the two proposals (see ref.<sup>[13]</sup> for details). The <sup>63</sup>Cu NMR spectra of **13** and **16** exhibit a single resonance at δ ≈ 0 ppm, indicating a similar environment for the copper atoms within these helicates. For **13**, this situation is consistent with only an (H-T) orientation of the ligands as was also found in its crystal structure. However, for **16**, we should theoretically observe two resonances with reference to an expected (H-H) orientation as observed in its crystal structure. In any case, these results are obviously not in agreement with the presence of a mixture of (H-H) and (H-T) conformers in which three resonances are normally expected. Considering this, we decided to perform low-temperature <sup>1</sup>H NMR ROESY experiments (233 K) on the copper dications **13**, **16**, silver dications **14**, **20** and zinc dication **23**.

In the case of zinc complex **23**, two inter-strand correlations were detected in the (298 K) <sup>1</sup>H NMR ROESY spectrum (Figure 8): one between the methyl protons of the bipyrazine unit and 7-H of the bipyridine unit and a second between methyl protons of the bipyridine unit and 1-H of the bipyrazine unit indicating a selective (H-T) orientation of the ligands in this complex. Unfortunately, in the case of the complexes **13**, **16** (copper), **14**, **20** (silver) and **18**, **21** (zinc), we were unable to freeze out the systems, because of a rapid exchange, which operated even at low temperature.

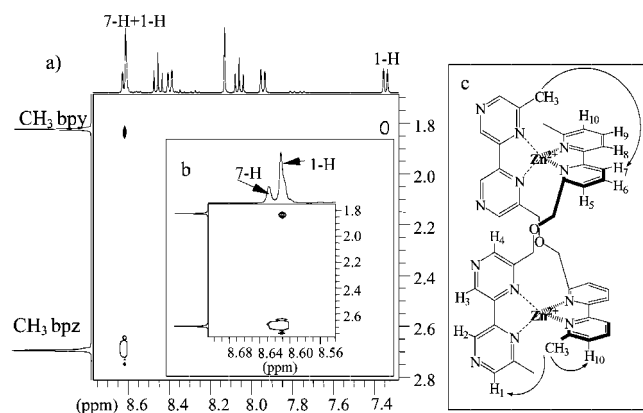


Figure 8. a) <sup>1</sup>H NMR ROESY of [Zn<sub>2</sub>(12)<sub>2</sub>][OTf]<sub>4</sub> (**23**) in CD<sub>3</sub>OD at 298 K (selected region); b) zoom on correlations between methyl and aromatic protons; c) scheme of the resulting double-stranded helicate structure (arrows indicate specific interactions)

Under these conditions, no correlation between terminal methyl protons of one heterocyclic unit and the aromatic protons of the opposite heterocyclic unit were observed by NMR spectroscopy.

### X-ray Structure Analysis

Finally, crystallized helicates [Ag<sub>2</sub>(11)<sub>2</sub>][PF<sub>6</sub>]<sub>2</sub> (**20**) and [Ag<sub>2</sub>(12)<sub>2</sub>][PF<sub>6</sub>]<sub>2</sub> (**22**) were obtained by slow diffusion of diethyl ether into acetonitrile solutions of the complexes (see Exp. Sect.) giving light yellow crystals suitable for X-ray crystallography. The two compounds both occupy the centrosymmetric *P* $\bar{1}$  space group with two PF<sub>6</sub><sup>-</sup> counterions in the asymmetric unit. An acetonitrile (C<sub>2</sub>H<sub>3</sub>N) solvent molecule was found in the asymmetric unit of **20**. However, the presence of PF<sub>6</sub> counterions induces, some disorder in the crystal packing and during the refinements.

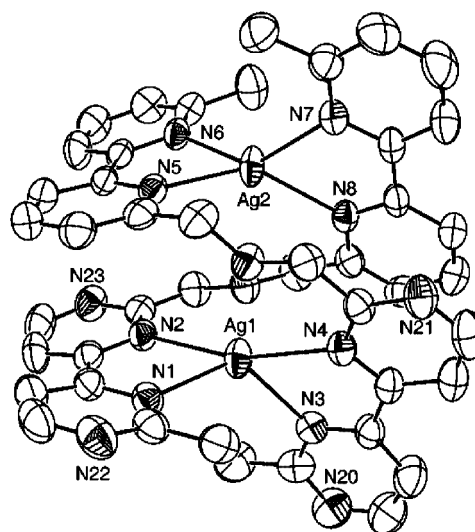


Figure 9. ORTEP drawing of the asymmetric unit of the silver complex [Ag<sub>2</sub>(11)<sub>2</sub>][PF<sub>6</sub>]<sub>2</sub> (**20**) (counterions and solvent molecules omitted); thermal ellipsoids are at 50% probability level

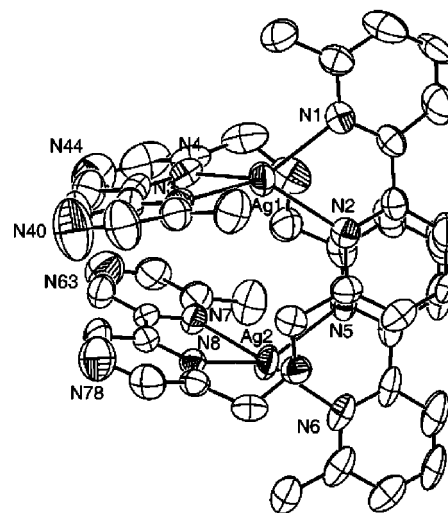


Figure 10. ORTEP drawing of the asymmetric unit of the silver complex [Ag<sub>2</sub>(12)<sub>2</sub>][PF<sub>6</sub>]<sub>2</sub> (**22**) (counterions omitted); thermal ellipsoids are at 50% probability level

The ORTEP<sup>[19]</sup> views of the two dinuclear Ag<sup>I</sup> complexes **20** and **22** are shown in Figures 9 and 10, respectively. As usual in the case of a chemical system with a large number of heavy atoms, it was impossible to observe all the hydrogen atoms in the Fourier difference maps. This made it particularly difficult to differentiate between N atoms and CH groups of the ligand nuclei without a careful inspection of C–C and C–N bond lengths and thermal displacements, which was done in this case. The complexes **20** and **22** are double-stranded helicates where each Ag<sup>I</sup> cation is in tetrahedral coordination involving the nitrogen atoms of the bipyrimidine (bpm), bipyrazine (bpz) and bipyridine (bpy) ligands. However, the complex **20** occupies an (H-H) conformation whereas the complex **22** is in an (H-T) conformation as shown in Figures 9 and 10. The intramolecular Ag–Ag distances are 4.14 and 6.13 Å for the complexes **20** and **22**, respectively. This large difference of 2 Å in the metal–metal spacing of the two helicates can be explained by the  $\pi$ -electronic interactions between the facing heteroatomic rings (bpm–bpy in complex **20** and bpz–bpz in complex **22**), which differ between the two complexes.

In the bpm–bpy interactions in **20**, the nitrogen atoms can avoid a close approach to the opposing  $\pi$ -electronic system.

More precisely, the nucleophilicity of the nitrogen atoms makes the N–N and the N– $\pi$ -electron repulsions highly involved and favour or disfavour the close approach of the heteroatomic nuclei and the attraction occurred. Conversely, electrostatic repulsion is dominant in the bpz–bpz facing heterocycles in **22**, especially because of the similar positions of the nitrogen atoms in the two facing rings. As a consequence of these interactions, the AgN<sub>4</sub> tetrahedra present distorted geometries as previously reported in our copper helicate studies.<sup>[5]</sup> The interatomic bond lengths and angles are given.<sup>[13]</sup> The average values of the Ag–N bond lengths for compound **20** are 2.406(5) Å [Ag(bpm)<sub>2</sub>], 2.339(5) Å [Ag(bpy)<sub>2</sub>] and are significantly longer than those in compound **22**, 2.321(7) Å [Ag(bpz–bpy)], 2.317(8) Å [Ag(bpz–bpy)], respectively. All N–Ag–N bond angles are within the range 70–140° except N2–Ag1–N4 = 163° found for the bpm interligand connection. Figures 11 and 12 depict the space-filling representations (MOLEKEL<sup>[20]</sup>

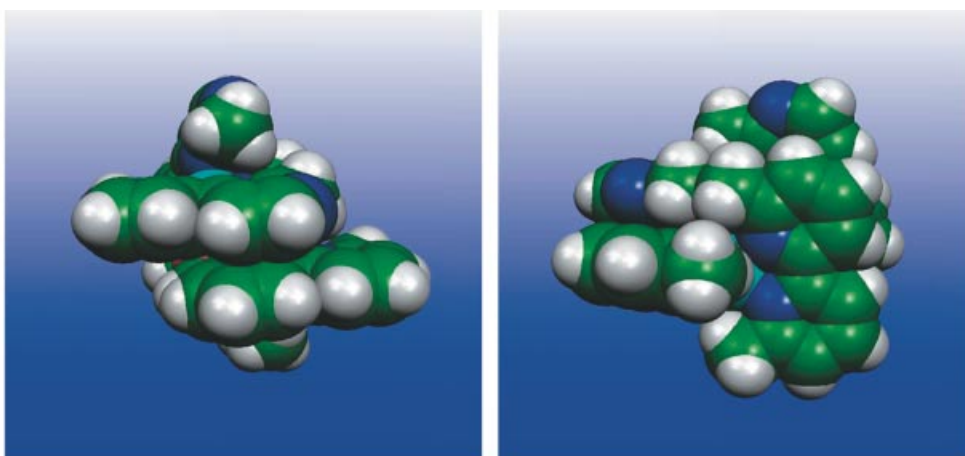


Figure 11. Two views of the space-filling representation of the silver helicate [Ag<sub>2</sub>(**11**)<sub>2</sub>][PF<sub>6</sub>]<sub>2</sub> (**20**) (N atoms blue)

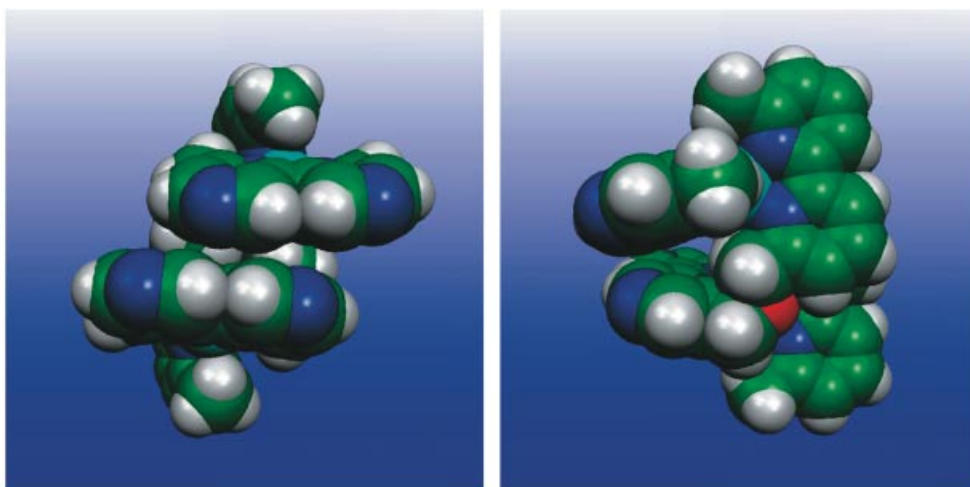


Figure 12. Two views of the space-filling representation of the silver helicate [Ag<sub>2</sub>(**12**)<sub>2</sub>][PF<sub>6</sub>]<sub>2</sub> (**22**) (N atoms blue, O atoms red)

visualization program) of the structures of **20** and **22** showing the interactions of heteroatomic ring packing and the N–N and N– $\pi$ -electron repulsions. In Figure 12, the bpm–bpy facing rings are close to each other. The stabilization of the facing rings imposes mutually transverse displacements.

The two helicates  $[\text{Cu}_2(\mathbf{9})_2][\text{PF}_6]_2$  (**13**) and  $[\text{Cu}_2(\mathbf{10})_2][\text{PF}_6]_2$  (**16**), were crystallized by slow diffusion of diethyl ether into acetonitrile or acetone solutions of the complexes (see Exp. Sect.). The resulting crystals were deep-red and fragile. The structures of the copper complexes **13** and **16** were determined from difficult X-ray single-crystal experiments (see Exp. Sect.) because of the poor quality of the crystals. Both compounds crystallized in the triclinic setting and the centrosymmetric  $P\bar{1}$  space group. Attempts to resolve and refine the structures in the  $P1$  space group did not improve their figures of merit and yielded high  $R$  values (see Exp. Sect.), which are expected for such disordered materials especially in the presence of  $\text{PF}_6^-$  counterions. Twinning was also considered but it was not observed in our samples. However, the helicate structures and conformations could be observed despite the complete disordering of the  $\text{PF}_6^-$  counterions in the crystal lattices. The asymmetric unit of **13** contains one dinuclear  $\text{Cu}^I$  complex, two  $\text{PF}_6^-$  counterions and one residual acetone ( $\text{C}_3\text{H}_6\text{O}$ ) solvent molecule. The complex **16** contains two dicopper(I) complexes and four  $\text{PF}_6^-$  counterions in the crystal asymmetric unit. The respective ORTEP<sup>[19]</sup> views of the two compounds are depicted in Figures 13 and 14, respectively.

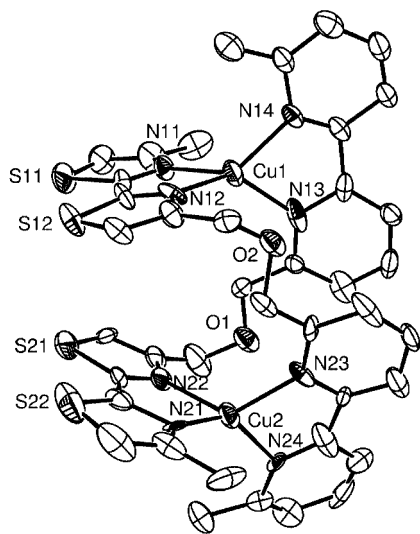


Figure 13. ORTEP drawing of the asymmetric unit of the copper complex  $[\text{Cu}_2(\mathbf{9})_2][\text{PF}_6]_2$  (**13**) (counterions and solvent molecules omitted); thermal ellipsoids are at 50% probability level

The intramolecular Cu–Cu distances are 5.95 Å (complex **13**) and 6.28 Å (helix **16a**) and 6.24 Å (helix **16b**). The dimetallic cations are double-stranded helicates yielding left- and right-handed units in the crystal because of the presence of the centre of inversion ( $P\bar{1}$  space group). It is worth noting that for complex **16**, both dinuclear **16a** and

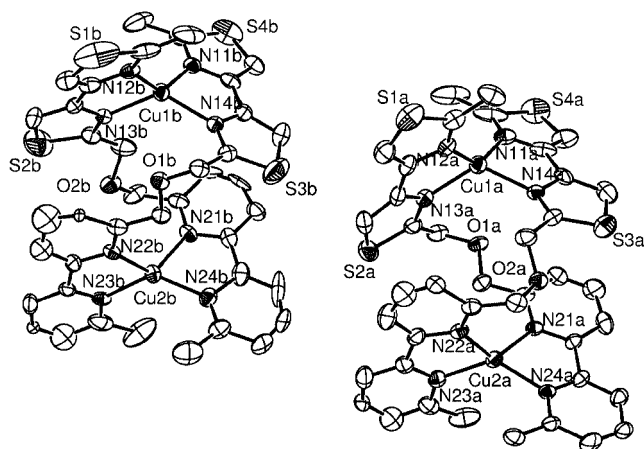


Figure 14. ORTEP drawing of the asymmetric unit contents of the copper complex  $[\text{Cu}_2(\mathbf{10})_2][\text{PF}_6]_2$  (**16**) (counterions and solvent molecules omitted); thermal ellipsoids are at 50% probability level

**16b** helices in the asymmetric unit have the same handedness (Figure 14). In the complexes **13** and **16**, the copper ions occupy a distorted tetrahedral coordination involving the nitrogen atoms of the bipyridine and bithiazole heterocyclic ligands. However, the position of the connecting carbon atoms (C-2 or -4) in the bithiazole rings is found to yield to either hetero-ligand (**13**) or homo-ligand (**16**) coordinations of the copper atom as shown in Figures 13 and 14. Consequently, a different ring stacking is obtained as shown in Figures 15 (**13**) and 16 (**16**) generated by the MOLEKEL<sup>[20]</sup> program. This stacking is due to the  $\pi$ – $\pi$  and electrostatic interactions between the heterocyclic ligands. Figures 15 and 16 indicate that these interactions are stronger when sulfur atoms are involved: the interactions become attractive. Both transverse and longitudinal displacements of facing heterocyclic ligand planes are observed. This obviously implies  $\text{CuN}_4$  distorted tetrahedral geometry especially when the copper atom is connected to one or two bithiazole ligands. These features were also reported in our previous study of the (bipyrazine–bipyridine)copper complex.<sup>[5]</sup> It is worth noting that the disorder of the  $\text{PF}_6^-$  counterions results in poor quality structure refinements and has an influence on the precision of the atomic bond lengths and angles in the organic part of the helicates. It can also distort the planarity of the ligand nuclei.

On the other hand, the geometry of the copper environment is much more stable because of the heavy metal contribution to the X-ray diffracting power of the samples. Atomic bond lengths and angles for copper coordination in compounds **13** and **16** are given in the Supporting Information.<sup>[13]</sup> All Cu–N bond lengths are approximately equal to 2 Å within the estimated error intervals. Similar bond angles in the range from 80° (intra-ligand angles) to 137° (interligand angles) are also found for the two compounds. We note that these structural values do not correlate with the nature of the heterocyclic ligand.

The X-ray structural analyses showed unambiguously that the discrete dinuclear copper helicates **13** and **16** were

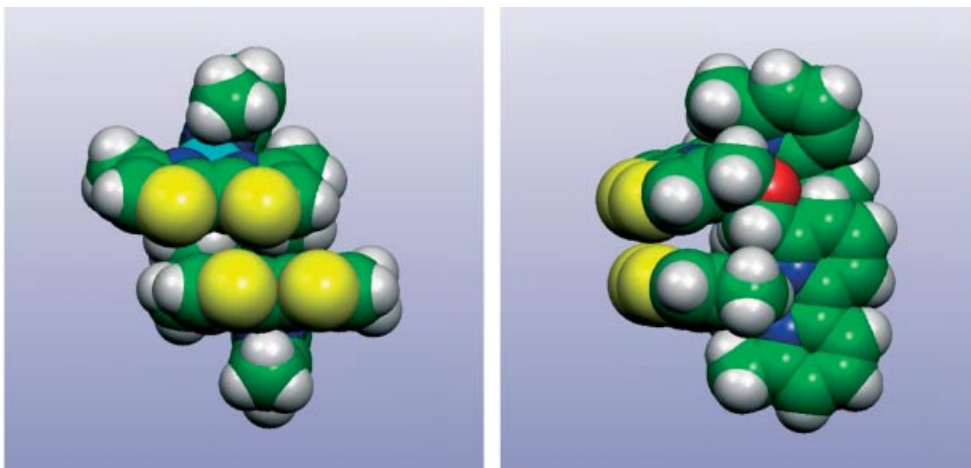


Figure 15. Two views of the space-filling representation of the copper helicate  $[\text{Cu}_2(\mathbf{9})_2][\text{PF}_6]_2$  (**13**) (S atoms yellow, O atoms red)

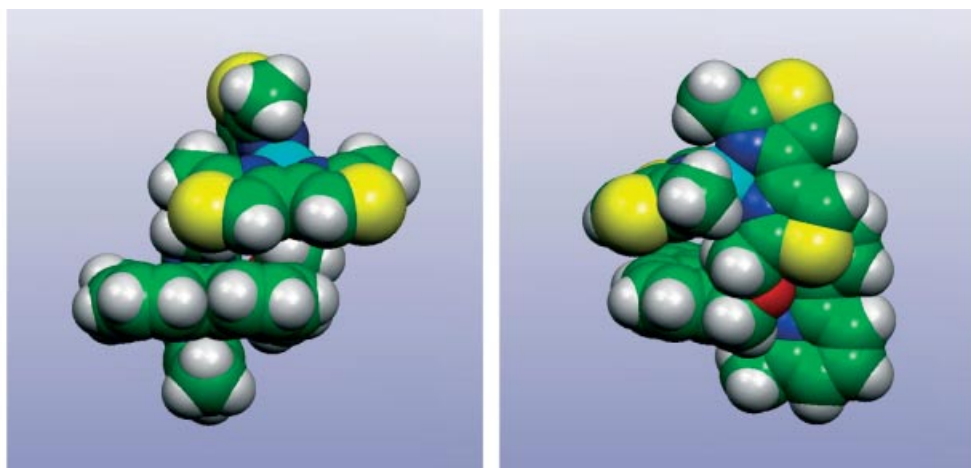


Figure 16. Two views of the space-filling representation of the copper helicate  $[\text{Cu}_2(\mathbf{10})_2][\text{PF}_6]_2$  (**16**) (S atoms yellow, O atoms red)

formed and adopt an (H-T) conformation with the bipyridine-2,2'-bithiazole heterotopic ligand and an (H-H) conformation with the bipyridine-4,4'-bithiazole heterotopic ligand. Both metal centres in the helicates are coordinated to the heterocyclic nitrogen atoms by a distorted tetrahedral geometry.

In unison with experimental<sup>[5]</sup> and theoretical<sup>[6]</sup> results obtained previously for the heterotopic bipyrazine–bipyridine ligand self-assembly process with  $\text{Cu}^{\text{I}}$ , an H-T conformation has also been obtained for this sequence with  $\text{Ag}^{\text{I}}$  and  $\text{Zn}^{\text{II}}$ . This “programming” was assigned to the electronic properties of the heterocycles on the basis of  $\text{Cu}^{\text{I}}$  orbital contributions to the HOMO and on the basis of a metal→ligand back-bonding phenomenon,<sup>[6]</sup> which enhances the stability of the hetero complex (bpz–bpy). Similar reasoning can be applied to the  $\text{Ag}^{\text{I}}$  and  $\text{Zn}^{\text{II}}$  metal complexes. Conversely, the bipyrimidine–bipyridine sequence **11** exhibits an H-H conformation. The only difference between the bipyrimidine and bipyrazine units lies in the heterocycle electronic configurations. As reported earlier by us,<sup>[24,25]</sup> both the reactivity and experimental electron density distribution of bipyrazine indicate its less aromatic character compared to other diazines such as bipyrimidine<sup>[26]</sup> and probably also to other diazines such as bipyridine or phenanthroline. Notably, the topological analysis of the electron density<sup>[24]</sup> allowed a comparison of the coordination scheme of the inner and outer nitrogen atoms of the bipyrazine and the 4,4'-bipyrimidine rings, respectively,<sup>[26]</sup> revealing a participation of the outer nitrogen atoms in the coordination of  $\text{Cu}^{\text{I}}$  only in the bipyrimidine ring. Unfortunately, ab initio DFT calculations on the 4,4'-bipyrimidine homo- and hetero- $\text{Cu}^{\text{I}}$  complexes failed and no data could be presented regarding this.

idine<sup>[26]</sup> and probably also to other diazines such as bipyridine or phenanthroline. Notably, the topological analysis of the electron density<sup>[24]</sup> allowed a comparison of the coordination scheme of the inner and outer nitrogen atoms of the bipyrazine and the 4,4'-bipyrimidine rings, respectively,<sup>[26]</sup> revealing a participation of the outer nitrogen atoms in the coordination of  $\text{Cu}^{\text{I}}$  only in the bipyrimidine ring. Unfortunately, ab initio DFT calculations on the 4,4'-bipyrimidine homo- and hetero- $\text{Cu}^{\text{I}}$  complexes failed and no data could be presented regarding this.

## Conclusion

In conclusion, we have demonstrated in this study that four different tetradentate heterotopic ligands containing 2,2-bipyrazine, 2,2'- or 4,4'-bithiazole or 4,4'-bipyrimidine fragments connected to a bipyridine nucleus are very effective for the spontaneous formation of new double-stranded head-to-head (H-H) or head-to-tail (H-T) fully oriented dinuclear helicates in the solid state. Analysis of the spectrophotometric UV/Vis titrations indicate that all the complexes are formed quantitatively at  $\text{M/L} = 1.0$  stoichi-

ometry and that the self-assembly process of the dinuclear double-stranded helicates is driven to completion by positive cooperativity.

However, it was not possible to ascertain the precise nature of the second species which appears in solution at lower temperature (especially in the cases of the silver and copper complexes) because of a very rapid dynamic interconversion equilibrium between conformers. Nevertheless, the structure of one zinc complex **23** with an H-T orientation was fully characterized, which indicates that the helical structures of the dinuclear metal complexes studied may persist in solution. This observation was made possible by the lack of exchange in that particular case.

Considering the X-ray structures of the four complexes, extensive heteroaromatic ring  $\pi$ -stacking and the overlap of near parallel fragments of adjacent ligands govern the metal–metal distance, modulate the pitch and bending of the helix shape and strongly stabilize the molecule. As a direct consequence of this, there is a remarkable and uncommon  $\text{Ag}^{\text{I}}$  cation distorted tetrahedral geometry in the corresponding helicate.

Finally, it is considered that “programming” oriented helicate self-assemblies could be achieved with a high efficiency by the design of heterotopic strands composed only of bis(heterocycles) with different electronic configurations in their structure. Projected investigations include: a) study of the role of the counter-anion in the formation and stability of helicates, b) study of the presented ligands’ complexation with hexacoordinating metal atoms. Further work is also in progress to use this property for the construction of other ligands and heterotopic sequences in order to programme novel supramolecularly oriented systems.

## Experimental Section

**General Remarks:**  $^1\text{H}$  and  $^{13}\text{C}$  NMR spectra were recorded with a Bruker DRX 400 spectrometer and  $^{63}\text{Cu}$  NMR spectra with a Bruker DRX 500 at  $-10\text{ }^\circ\text{C}$ , UV/Vis spectra were recorded with a Uvmc2 Safas spectrophotometer. Mass spectra (ES) were taken with a Micromass Platform spectrometer. Elemental analyses were obtained with a Perkin–Elmer 240C CHN-O-S analyzer. Solvents were purified by standard methods.

**2-(Bromomethyl)-2'-methyl-4,4'-bithiazole (4):** NBS (998 mg, 5.61 mmol) was added to a solution of 6,6'-dimethyl-4,4'-bithiazole<sup>[9]</sup> (1 g, 5.10 mmol) in  $\text{CCl}_4$  (100 mL) under Ar. The mixture was refluxed for 30 min, then benzoyl peroxide (85 mg) was added. The mixture was refluxed and irradiated with a tungsten lamp (100 W) for 45 min. The resulting mixture was cooled to  $0\text{ }^\circ\text{C}$  and the precipitate was filtered, washed with  $\text{CH}_2\text{Cl}_2$ , and the solvent was removed in vacuo. The crude product was purified by chromatography on silica gel (elution:  $\text{CH}_2\text{Cl}_2/\text{acetone}$ , 95:5). Yield: 708 mg (50%). M.p.  $128\text{ }^\circ\text{C}$ .  $^1\text{H}$  NMR (400 MHz,  $\text{CDCl}_3$ ,  $25\text{ }^\circ\text{C}$ ):  $\delta = 7.78$  (s, 1  $\text{H}_{\text{Ar}}$ ), 7.62 (s, 1  $\text{H}_{\text{Ar}}$ ), 4.77 (s, 2 H), 2.76 (s, 3 H) ppm.  $^{13}\text{C}$  NMR (100 MHz,  $\text{CDCl}_3$ ,  $25\text{ }^\circ\text{C}$ ):  $\delta = 166.4$  (q), 165.8 (q), 150.8 (q), 149.6 (q), 116.9 ( $\text{CH}_{\text{Ar}}$ ), 115.2 ( $\text{CH}_{\text{Ar}}$ ), 26.6 ( $\text{CH}_2\text{Br}$ ), 19.2 ( $\text{CH}_3$ ) ppm.  $\text{C}_8\text{H}_7\text{BrN}_2\text{S}_2$  (275.19): calcd. C 34.92, H 2.56, N 10.18; found C 34.9, H 2.54, N 10.12.

**2-(Bromomethyl)-2'-methyl-4,4'-bipyrimidine (6):** NBS (688 mg, 3.86 mmol) and AIBN were added to a solution of 2,2'-dimethyl-4,4'-bipyrimidine (1.2 g, 6.44 mmol) in  $\text{CCl}_4$  (50 mL) under Ar. The mixture was refluxed and irradiated with a tungsten lamp (100 W) for 4 h. The resulting precipitate was filtered, washed with  $\text{CH}_2\text{Cl}_2$ , and the solvent was removed in vacuo. The crude product was purified by chromatography on silica gel (elution:  $\text{CH}_2\text{Cl}_2/\text{Et}_2\text{O}$ , 75:25), which gave **6** as a white powder. Yield: 480 mg (28%).  $^1\text{H}$  NMR (400 MHz,  $\text{CDCl}_3$ ,  $25\text{ }^\circ\text{C}$ ):  $\delta = 8.94$  (d,  $^3J = 5.1$  Hz, 1  $\text{H}_{\text{Ar}}$ ), 8.85 (d,  $^3J = 4.9$  Hz, 1  $\text{H}_{\text{Ar}}$ ), 8.32 (d,  $^3J = 5.1$  Hz, 1  $\text{H}_{\text{Ar}}$ ), 8.24 (d,  $^3J = 5.2$  Hz, 1  $\text{H}_{\text{Ar}}$ ), 4.69 (s, 2 H,  $\text{CH}_2\text{Br}$ ), 2.83 (s, 3 H,  $\text{CH}_3$ ) ppm.  $^{13}\text{C}$  NMR (100 MHz,  $\text{CDCl}_3$ ,  $25\text{ }^\circ\text{C}$ ):  $\delta = 168.5$  (q), 166.4 (q), 161.9 (q), 160.4 (q), 159.3 ( $\text{CH}_{\text{Ar}}$ ), 158.7 ( $\text{CH}_{\text{Ar}}$ ), 116.1 ( $\text{CH}_{\text{Ar}}$ ), 114.8 ( $\text{CH}_{\text{Ar}}$ ), 33.6 ( $\text{CH}_2\text{Br}$ ), 26.1 ( $\text{CH}_3$ ) ppm.

**6'-Methyl-6-[(4'-methyl-2,2'-bithiazol-4-yl)methoxy]methyl]-2,2'-bipyridine (9):** 6-(Hydroxymethyl)-6'-methyl-2, 2'-bipyridine (300 mg, 1.50 mmol) in THF (10 mL) was added to a suspension of NaH (72 mg, 3.00 mmol) in anhydrous THF (5 mL) under Ar at  $0\text{ }^\circ\text{C}$ . The mixture was stirred at  $0\text{ }^\circ\text{C}$  for 1 h, then 6-(bromomethyl)-6'-methyl-2, 2'-bithiazole (413 mg, 1.50 mmol) in THF (10 mL) was added, and the mixture was warmed to room temperature. The mixture was stirred at  $40\text{ }^\circ\text{C}$  for 4 h. After cooling to room temperature,  $\text{H}_2\text{O}$  (10 mL) was added to the mixture and the phases were separated. The aqueous layer was extracted with  $\text{CH}_2\text{Cl}_2$  ( $3 \times 30$  mL). The combined organic phases were dried with  $\text{MgSO}_4$  and the solvent was removed in vacuo. The solid was purified by chromatography on silica gel (elution:  $\text{CH}_2\text{Cl}_2$ ). Yield: 490 mg (83%). M.p.  $118\text{ }^\circ\text{C}$ .  $^1\text{H}$  NMR (400 MHz,  $\text{CDCl}_3$ ,  $25\text{ }^\circ\text{C}$ ):  $\delta = 8.32$  (d,  $^3J = 7.8$  Hz, 1  $\text{H}_{\text{Ar}}$  bpy), 8.19 (d,  $^3J = 7.6$  Hz, 1  $\text{H}_{\text{Ar}}$  bpy), 7.83 (t,  $^3J = 7.8$  Hz, 1  $\text{H}_{\text{Ar}}$  bpy), 7.69 (t,  $^3J = 7.6$  Hz, 1  $\text{H}_{\text{Ar}}$  bpy), 7.53 (d,  $^3J = 7.6$  Hz, 1  $\text{H}_{\text{Ar}}$  bpy), 7.41 (s, 1  $\text{H}_{\text{Ar}}$  btz), 7.16 (d,  $^3J = 7.6$  Hz, 1  $\text{H}_{\text{Ar}}$  bpy), 6.98 (s, 1  $\text{H}_{\text{Ar}}$  bpy), 4.89 (s, 2 H,  $\text{CH}_2$ , btz), 4.87 (s, 2 H,  $\text{CH}_2$ , bpy), 2.63 (s, 3 H,  $\text{CH}_3$ , bpy), 2.51 (s, 3 H,  $\text{CH}_3$ , btz) ppm.  $^{13}\text{C}$  NMR (100 MHz,  $\text{CDCl}_3$ ,  $25\text{ }^\circ\text{C}$ ):  $\delta = 161.6$  (q, bpy), 160.4 (q, bpy), 157.8 (q, bpy), 157.5 (q, bpy), 155.8 (q, btz), 155.5 (q, btz), 155.0 (q, btz), 154.1 (q, btz), 137.4 ( $\text{CH}_{\text{Ar}}$  bpy), 137.0 ( $\text{CH}_{\text{Ar}}$  bpy), 123.2 ( $\text{CH}_{\text{Ar}}$  bpy), 121.1 ( $\text{CH}_{\text{Ar}}$  bpy), 119.8 ( $\text{CH}_{\text{Ar}}$  bpy), 118.1 ( $\text{CH}_{\text{Ar}}$  bpy), 117.6 ( $\text{CH}_{\text{Ar}}$  btz), 115.7 ( $\text{CH}_{\text{Ar}}$  btz), 73.8 ( $\text{CH}_2$ , btz), 68.6 ( $\text{CH}_2$ , bpy), 24.6 ( $\text{CH}_3$ , bpy), 17.1 ( $\text{CH}_3$ , btz) ppm. UV/Vis ( $\text{CH}_3\text{CN}$ ):  $\lambda_{\text{max}}$ . ( $\epsilon_{\text{max}}$ ) = 290 (19500), 328 (14450) nm.  $\text{C}_{20}\text{H}_{18}\text{N}_4\text{OS}_2 \cdot 0.25\text{CH}_2\text{Cl}_2$  (415.74): calcd. C 58.50, H 4.49, N 13.48; found C 58.31, H 4.47, N 13.26.

**6'-Methyl-6-[(2'-methyl-4,4'-bithiazol-2-yl)methoxy]methyl]-2,2'-bipyridine (10):** 6-(Hydroxymethyl)-6'-methyl-2,2'-bipyridine (268 mg, 1.34 mmol) in THF (10 mL) was added to a suspension of NaH (65 mg, 2.68 mmol) in anhydrous THF (5 mL) under Ar at  $0\text{ }^\circ\text{C}$ . The mixture was stirred at  $0\text{ }^\circ\text{C}$  for 1 h, then 6-(bromomethyl)-6'-methyl-4,4'-bithiazole (369 mg, 1.34 mmol) in THF (10 mL) was added, and the mixture was allowed to warm to room temperature. The mixture was stirred at  $40\text{ }^\circ\text{C}$  for 4 h. After cooling to room temperature,  $\text{H}_2\text{O}$  (10 mL) was added to the mixture and the phases were separated. The aqueous layer was extracted with  $\text{CH}_2\text{Cl}_2$  ( $3 \times 30$  mL). The combined organic phases were dried with  $\text{MgSO}_4$  and the solvent was removed in vacuo. The solid was purified by chromatography on silica gel (elution:  $\text{CH}_2\text{Cl}_2$ ). Yield: 437 mg (83%). M.p.  $156\text{ }^\circ\text{C}$ .  $^1\text{H}$  NMR (400 MHz,  $\text{CDCl}_3$ ,  $25\text{ }^\circ\text{C}$ ):  $\delta = 8.34$  (d,  $^3J = 7.4$  Hz, 1  $\text{H}_{\text{Ar}}$  bpy), 8.19 (d,  $^3J = 7.4$  Hz, 1  $\text{H}_{\text{Ar}}$  bpy), 7.84 (t,  $^3J = 7.6$  Hz, 1  $\text{H}_{\text{Ar}}$  bpy), 7.76 (s, 1  $\text{H}_{\text{Ar}}$  btz), 7.68 (d,  $^3J = 7.2$  Hz, 1  $\text{H}_{\text{Ar}}$  bpy), 7.60 (s, 1  $\text{H}_{\text{Ar}}$  btz), 7.53 (d,  $^3J = 7.2$  Hz, 1  $\text{H}_{\text{Ar}}$  bpy), 7.16 (d,  $^3J = 7.2$  Hz, 1  $\text{H}_{\text{Ar}}$  bpy), 5.03 (s, 2 H,  $\text{CH}_2$ , btz), 4.92 (s, 2 H,  $\text{CH}_2$ , bpy), 2.76 (s, 3 H,  $\text{CH}_3$ , btz), 2.64 (s, 3 H,  $\text{CH}_3$ , bpy) ppm.  $^{13}\text{C}$  NMR (100 MHz,  $\text{CDCl}_3$ ,  $25\text{ }^\circ\text{C}$ ):  $\delta = 168.8$

(q, bpy), 166.3 (q, btz), 157.8 (q, bpy), 157.0 (q, bpy), 155.8 (q, bpy), 155.4 (q, bpy), 150.5 (q, btz), 150.1 (q, btz), 137.5 (CH<sub>AB</sub>, bpy), 136.9 (CH<sub>AB</sub>, bpy), 123.2 (CH<sub>AB</sub>, bpy), 121.1 (CH<sub>AB</sub>, bpy), 119.9 (CH<sub>AB</sub>, bpy), 118.1 (CH<sub>AB</sub>, bpy), 115.2 (CH<sub>AB</sub>, btz), 114.7 (CH<sub>AB</sub>, btz), 74.1 (CH<sub>2</sub>, btz), 69.7 (CH<sub>2</sub>, bpy), 24.6 (CH<sub>3</sub>, bpy), 19.2 (CH<sub>3</sub>, btz) ppm. UV/Vis (CH<sub>3</sub>CN): λ<sub>max</sub>. (ε<sub>max</sub>.) = 265 (21100), 287 (18100) nm. C<sub>20</sub>H<sub>18</sub>N<sub>4</sub>OS<sub>2</sub>·1/7CH<sub>2</sub>Cl<sub>2</sub> (406.65): calcd. C 59.49, H 4.53, N 13.78; found C 59.46, H 4.53, N 13.59.

**6'-Methyl-6-[(2'-methyl-4,4'-bipyrimidin-2-yl)methoxy]methyl]-2,2'-bipyridine (11):** 6-(Hydroxymethyl)-6'-methyl-2,2'-bipyridine (348 mg, 1.74 mmol) was added to a suspension of NaH (84 mg, 3.50 mmol) in anhydrous THF (30 mL) under Ar at 0 °C. The mixture was stirred at 0 °C for 1 h, then 2-(bromomethyl)-2'-methyl-4,4'-bipyrimidine (461 mg, 1.74 mmol) was added, and the mixture was allowed to warm to room temperature. The mixture was stirred at 40 °C for 2 h. After cooling to room temperature, H<sub>2</sub>O (10 mL) was added to the mixture and the phases were separated. The aqueous layer was extracted with CH<sub>2</sub>Cl<sub>2</sub> (3 × 30 mL). The combined organic phases were dried with MgSO<sub>4</sub>, and the solvent was removed in vacuo. The crude product was purified by chromatography on aluminium oxide gel (elution: CH<sub>2</sub>Cl<sub>2</sub>), and gave a white powder. Yield 500 mg (75%). M.p. 152 °C. <sup>1</sup>H NMR (400 MHz, CDCl<sub>3</sub>, 25 °C): δ = 8.99 (d, <sup>3</sup>J = 5.1 Hz, 1 H<sub>AB</sub>, bpm), 8.82 (d, <sup>3</sup>J = 5.1 Hz, 1 H<sub>AB</sub>, bpm), 8.35 (d, <sup>3</sup>J = 4.9 Hz, 1 H<sub>AB</sub>, bpm), 8.33 (d, <sup>3</sup>J = 8.0 Hz, 1 H<sub>AB</sub>, bpy), 8.24 (d, <sup>3</sup>J = 4.9 Hz, 1 H<sub>AB</sub>, bpm), 8.20 (d, <sup>3</sup>J = 7.8 Hz, 1 H<sub>AB</sub>, bpy), 7.86 (t, <sup>3</sup>J = 7.8 Hz, 1 H<sub>AB</sub>, bpy), 7.69 (t, <sup>3</sup>J = 7.6 Hz, 1 H<sub>AB</sub>, bpy), 7.64 (d, <sup>3</sup>J = 7.6 Hz, 1 H<sub>AB</sub>, bpy), 7.18 (d, <sup>3</sup>J = 7.6 Hz, 1 H<sub>AB</sub>, bpy), 5.04 (s, 2 H, OCH<sub>2</sub>, bpm), 5.03 (s, 2 H, OCH<sub>2</sub>, bpy), 2.85 (s, 3 H, CH<sub>3</sub>, bpm), 2.65 (s, 3 H, CH<sub>3</sub>, bpy) ppm. <sup>13</sup>C NMR (100 MHz, CDCl<sub>3</sub>, 25 °C): δ = 168.4 (q, bpm), 167.2 (q, bpm), 161.4 (q, bpm), 160.7 (q, bpm), 159.0 (CH<sub>AB</sub>, bpm), 158.6 (CH<sub>AB</sub>, bpm), 157.8 (q, bpy), 157.6 (q, bpy), 155.8 (q, bpy), 155.5 (q, bpy), 137.4 (CH<sub>AB</sub>, bpy), 136.9 (CH<sub>AB</sub>, bpy), 123.1 (CH<sub>AB</sub>, bpy), 121.3 (CH<sub>AB</sub>, bpy), 119.8 (CH<sub>AB</sub>, bpy), 118.1 (CH<sub>AB</sub>, bpy), 116.0 (CH<sub>AB</sub>, bpm), 114.7 (CH<sub>AB</sub>, bpm), 74.4 (OCH<sub>2</sub>, bpy), 73.5 (OCH<sub>2</sub>, bpm), 26.0 (CH<sub>3</sub>, bpm), 24.6 (CH<sub>3</sub>, bpy) ppm. UV/Vis (CH<sub>3</sub>CN): λ<sub>max</sub>. (ε) = 285 (25117) nm. C<sub>22</sub>H<sub>20</sub>N<sub>6</sub>O·1/9CH<sub>2</sub>Cl<sub>2</sub> (393.87): calcd. C 67.43, H 5.17, N 21.34; found C 67.4, H 5.19, N 21.33.

**Compound 12:** Data see ref.<sup>[5]</sup>

**[Cu<sub>2</sub>(9)<sub>2</sub>][PF<sub>6</sub>]<sub>2</sub> (13):** [Cu(CH<sub>3</sub>CN)<sub>4</sub>][PF<sub>6</sub>] (190 mg, 0.51 mmol) was added to the ligand **9** (200 mg, 0.51 mmol) dissolved in anhydrous CH<sub>3</sub>CN (50 mL) under Ar. The mixture was stirred at room temperature and instantly yielding a deep-red solution. After evaporation of the solvent, the solid residue was crystallised by slow diffusion of diethyl ether into an acetone solution which gave deep-red crystals. Yield 98%. <sup>1</sup>H NMR (A/B = 64:36; 400 MHz, CD<sub>3</sub>CN, -30 °C): δ = 8.28 (d, <sup>3</sup>J = 8.0 Hz, 1 H<sub>AB</sub>, bpy<sub>A</sub>), 8.23–8.16 (m, 1 H<sub>AB</sub>, bpy<sub>A</sub>, 2 H<sub>AB</sub>, bpy<sub>B</sub>), 8.11 (t, <sup>3</sup>J = 7.8 Hz, 1 H<sub>AB</sub>, bpy<sub>B</sub>), 8.07 (t, <sup>3</sup>J = 7.8 Hz, 1 H<sub>AB</sub>, bpy<sub>A</sub>), 8.01 (t, <sup>3</sup>J = 7.8 Hz, 1 H<sub>AB</sub>, bpy<sub>B</sub>), 7.92 (t, <sup>3</sup>J = 7.8 Hz, 1 H<sub>AB</sub>, bpy<sub>A</sub>), 7.81 (d, <sup>3</sup>J = 7.4 Hz, 1 H<sub>AB</sub>, bpy<sub>B</sub>), 7.64 (d, <sup>3</sup>J = 7.2 Hz, 1 H<sub>AB</sub>, bpy<sub>A</sub>), 7.63 (s, 1 H<sub>AB</sub>, btz<sub>B</sub>), 7.58 (d, <sup>3</sup>J = 7.2 Hz, 1 H<sub>AB</sub>, bpy<sub>B</sub>), 7.37 (d, <sup>3</sup>J = 7.6 Hz, 1 H<sub>AB</sub>, bpy<sub>A</sub>), 7.24 (s, 1 H<sub>AB</sub>, btz<sub>B</sub>), 7.21 (s, 1 H<sub>AB</sub>, btz<sub>A</sub>), 7.01 (s, 1 H<sub>AB</sub>, btz<sub>A</sub>), 4.99 (s, 2 H, OCH<sub>2</sub>, bpy<sub>B</sub>), 4.86 (s, 2 H, OCH<sub>2</sub>, btz<sub>B</sub>), 4.31–4.22 (“q”, J<sub>AB</sub> = 12.8 Hz, 2 H, OCH<sub>2</sub>, bpy<sub>A</sub>), 4.20–4.13 (“q”, J<sub>AB</sub> = 13.7 Hz, 2 H, OCH<sub>2</sub>, btz<sub>A</sub>), 2.80 (s, 3 H, CH<sub>3</sub>, bpy<sub>B</sub>), 2.48 (s, 3 H, CH<sub>3</sub>, bpy<sub>A</sub>), 2.45 (s, 3 H, CH<sub>3</sub>, btz<sub>B</sub>), 2.05 (s, 3 H, CH<sub>3</sub>, btz<sub>A</sub>) ppm. <sup>13</sup>C NMR (100 MHz, CD<sub>3</sub>CN, -30 °C): δ = 160.7 (q, bpy<sub>B</sub>), 160.5 (q, bpy<sub>A</sub>, q, bpy<sub>B</sub>), 159.1 (q, bpy<sub>A</sub>), 157.2 (q, bpy<sub>B</sub>), 156.7 (q, bpy<sub>A</sub>), 156.5 (q, bpy<sub>B</sub>), 155.7 (q, bpy<sub>A</sub>), 153.4 (q, btz<sub>A</sub>, q, btz<sub>B</sub>), 153.2 (q, btz<sub>B</sub>), 152.8 (q, btz<sub>A</sub>), 150.8 (q, btz<sub>A</sub>), 150.5

(q, btz<sub>B</sub>), 150.0 (q, btz<sub>A</sub>), 149.9 (q, btz<sub>B</sub>), 138.6 (CH<sub>AB</sub>, bpy<sub>B</sub>), 138.2 (CH<sub>AB</sub>, bpy<sub>B</sub>), 138.1 (CH<sub>AB</sub>, bpy<sub>A</sub>), 137.7 (CH<sub>AB</sub>, bpy<sub>A</sub>), 125.4 (CH<sub>AB</sub>, bpy<sub>B</sub>), 125.3 (CH<sub>AB</sub>, bpy<sub>A</sub>), 123.2 (CH<sub>AB</sub>, bpy<sub>A</sub>), 122.4 (CH<sub>AB</sub>, bpy<sub>B</sub>), 120.4 (CH<sub>AB</sub>, bpy<sub>A</sub>), 120.0 (CH<sub>AB</sub>, bpy<sub>B</sub>), 119.2 (CH<sub>AB</sub>, bpy<sub>B</sub>), 118.9 (CH<sub>AB</sub>, bpy<sub>A</sub>), 118.7 (CH<sub>AB</sub>, btz<sub>B</sub>), 118.3 (CH<sub>AB</sub>, btz<sub>A</sub>), 116.3 (CH<sub>AB</sub>, btz<sub>B</sub>), 116.1 (CH<sub>AB</sub>, btz<sub>A</sub>), 71.5 (OCH<sub>2</sub>, bpy<sub>B</sub>), 71.1 (OCH<sub>2</sub>, bpy<sub>A</sub>), 67.2 (OCH<sub>2</sub>, btz<sub>B</sub>), 66.7 (OCH<sub>2</sub>, btz<sub>A</sub>), 29.5 (CH<sub>3</sub>, bpy<sub>B</sub>), 24.2 (CH<sub>3</sub>, btz<sub>B</sub>), 23.7 (CH<sub>3</sub>, bpy<sub>A</sub>), 15.5 (CH<sub>3</sub>, btz<sub>A</sub>) ppm. UV/Vis (CH<sub>3</sub>CN): λ<sub>max</sub>. (ε<sub>max</sub>.) = 302, (20200), 450 (MLCT) (1720) nm. ESMS: m/z (%) = 1060.7 (60) [Cu<sub>2</sub>(9)<sub>2</sub>(PF<sub>6</sub><sup>-</sup>)<sup>+</sup>, 851.0 (80) [Cu<sub>2</sub>(9)<sup>+</sup>, 457.0 (100) [Cu<sub>2</sub>(9)<sub>2</sub>]<sup>2+</sup>/2. C<sub>40</sub>H<sub>36</sub>Cu<sub>2</sub>F<sub>12</sub>N<sub>8</sub>O<sub>2</sub>P<sub>2</sub>S<sub>4</sub>·CH<sub>2</sub>Cl<sub>2</sub>·H<sub>2</sub>O (1309.00): calcd. C 37.62, H 3.08, N 8.56; found C 37.78, H 2.95, N 8.57.

**[Ag<sub>2</sub>(9)<sub>2</sub>][PF<sub>6</sub>]<sub>2</sub> (14):** AgPF<sub>6</sub> (64.2 mg, 0.25 mmol) was added to the ligand **9** (100 mg, 0.25 mmol) dissolved in anhydrous CH<sub>3</sub>CN (20 mL) under Ar. The mixture was stirred at room temperature and after evaporation of the solvent, the solid residue was crystallised by slow diffusion of diethyl ether into an acetone solution which gave white crystals. Yield 99%. <sup>1</sup>H NMR (400 MHz, CD<sub>3</sub>CN, 25 °C): δ = 8.90 (2 d, 2H<sub>AB</sub>, bpy), 8.08 (t, <sup>3</sup>J = 7.8 Hz, 1 H<sub>AB</sub>, bpy), 7.91 (t, <sup>3</sup>J = 7.8 Hz, 1 H<sub>AB</sub>, bpy), 7.49 (d, <sup>3</sup>J = 7.6 Hz, 1 H<sub>AB</sub>, bpy), 7.39 (d, 1 H<sub>AB</sub>, bpy), 7.38 (s, 1 H<sub>AB</sub>, btz), 7.30 (s, 1 H<sub>AB</sub>, btz), 4.56 (s, 4 H, OCH<sub>2</sub>, bpy, OCH<sub>2</sub>, btz), 2.55 (s, 3 H, CH<sub>3</sub>, bpy), 2.38 (s, 3 H, CH<sub>3</sub>, btz) ppm. <sup>13</sup>C NMR (100 MHz, CD<sub>3</sub>CN, 25 °C): δ = 161.2 (q, bpy), 158.4 (q, bpy), 158.3 (q, bpy), 156.2 (q, bpy), 153.9 (q, btz), 152.6 (q, btz), 151.1 (q, btz), 150.4 (q, bpy), 139.4 (CH<sub>AB</sub>, bpy), 139.6 (CH<sub>AB</sub>, bpy), 125.4 (CH<sub>AB</sub>, bpy), 123.7 (CH<sub>AB</sub>, bpy), 121.6 (CH<sub>AB</sub>, bpy), 119.9 (CH<sub>AB</sub>, bpy), 119.5 (CH<sub>AB</sub>, btz), 117.5 (CH<sub>AB</sub>, btz), 72.4 (OCH<sub>2</sub>, bpy), 66.9 (OCH<sub>2</sub>, btz), 25.8 (CH<sub>3</sub>, bpy), 15.9 (CH<sub>3</sub>, btz) ppm. UV/Vis (CH<sub>3</sub>CN): λ<sub>max</sub>. (ε<sub>max</sub>.) = 300 (18800), 328 (12800) nm. ESMS: m/z (%) = 501.2 (60) [Ag<sub>2</sub>(9)<sub>2</sub>]<sup>2+</sup>/2. C<sub>40</sub>H<sub>36</sub>Ag<sub>2</sub>F<sub>12</sub>N<sub>8</sub>O<sub>2</sub>P<sub>2</sub>S<sub>4</sub>·5/2 CHCl<sub>3</sub>·0.5H<sub>2</sub>O (1602.30): calcd. C 31.86, H 2.49, N 6.99; found C 31.58, H 2.44, N 7.28.

**[Zn<sub>2</sub>(9)<sub>2</sub>][OTf]<sub>4</sub> (15):** Zn(OTf)<sub>2</sub> (28.2 mg, 0.076 mmol) was added to the ligand **9** (30 mg, 0.076 mmol) dissolved in CH<sub>3</sub>OH (10 mL) under Ar. The mixture was stirred at room temperature for 1 h and the solvent was evaporated. Yield 99%. <sup>1</sup>H NMR (400 MHz, CD<sub>3</sub>OD, 25 °C): δ = 8.76 (d, <sup>3</sup>J = 8.0 Hz, 1 H<sub>AB</sub>, bpy), 8.61 (d, <sup>3</sup>J = 8.0 Hz, 1 H<sub>AB</sub>, bpy), 8.49 (t, <sup>3</sup>J = 8.0 Hz, 1 H<sub>AB</sub>, bpy), 8.20 (t, <sup>3</sup>J = 8.0 Hz, 1 H<sub>AB</sub>, bpy), 7.98 (d, <sup>3</sup>J = 7.8 Hz, 1 H<sub>AB</sub>, bpy), 7.56 (d, <sup>3</sup>J = 7.8 Hz, 1 H<sub>AB</sub>, bpy), 7.27 (s, 1 H<sub>Ar</sub>, btz), 7.25 (s, 1 H<sub>Ar</sub>, btz), 5.41–5.27 (“q”, AB, J<sub>AB</sub> = 15.2 Hz, 2 H, OCH<sub>2</sub>, bpy), 4.30–4.09 (“q”, AB, J<sub>AB</sub> = 13.4 Hz, 2 H, OCH<sub>2</sub>, btz), 2.48 (s, 3 H, CH<sub>3</sub>, btz), 1.95 (s, 3 H, CH<sub>3</sub>, bpy) ppm. <sup>13</sup>C NMR (100 MHz, CD<sub>3</sub>OD, 25 °C): δ = 162.4 (q, bpy), 159.8 (q, bpy), 157.0 (q, bpy), 154.7 (q, bpy), 148.5 (2 q, btz), 148.2 (2 q, btz), 143.6 (CH<sub>AB</sub>, bpy), 142.8 (CH<sub>AB</sub>, bpy), 129.0 (CH<sub>AB</sub>, bpy), 125.4 (CH<sub>AB</sub>, bpy), 122.9 (CH<sub>AB</sub>, bpy), 121.6 (CH<sub>AB</sub>, bpy), 121.3 (CH<sub>AB</sub>, btz), 116.8 (CH<sub>AB</sub>, btz), 68.5 (OCH<sub>2</sub>, bpy), 67.5 (OCH<sub>2</sub>, btz), 22.3 (CH<sub>3</sub>, bpy), 15.9 (CH<sub>3</sub>, btz) ppm. UV/Vis (CH<sub>3</sub>OH): λ<sub>max</sub>. (ε) = 250 (9180), 312 (26062) nm. ESIMS: m/z (%) = 1364.0 (36) [Zn<sub>2</sub>(9)<sub>2</sub>(OTf)<sub>3</sub>]<sup>+</sup>, 1001.0 (19) [Zn(9)<sub>2</sub>(OTf)]<sup>+</sup>, 607.0 (72) [Zn<sub>2</sub>(9)<sub>2</sub>(OTf)<sub>2</sub>]<sup>2+</sup>/2, 426.2 (100) [Zn(9)<sub>2</sub>]<sup>2+</sup>/2, 229.0 (35) [Zn<sub>2</sub>(9)<sub>2</sub>]<sup>4+</sup>/4.

**[Cu<sub>2</sub>(10)<sub>2</sub>][PF<sub>6</sub>]<sub>2</sub> (16):** [Cu(CH<sub>3</sub>CN)<sub>4</sub>][PF<sub>6</sub>] (190 mg, 0.51 mmol) was added to the ligand **10** (200 mg, 0.51 mmol) dissolved in anhydrous CH<sub>3</sub>CN (50 mL) under Ar. The mixture was stirred at room temperature and instantly yielding a deep-orange solution. After evaporation of the solvent, the solid residue was crystallised by slow diffusion of diethyl ether into an acetonitrile solution which gave deep-orange crystals. Yield 92%. <sup>1</sup>H NMR (A/B = 51:49; 400 MHz, CD<sub>3</sub>CN, -40 °C): δ = 8.34–8.26 (m, 3 H<sub>Ar</sub>), 8.27 (d, <sup>3</sup>J = 7.8 Hz, 1 H<sub>Ar</sub>, bpy), 8.20–8.11 (m, 4 H<sub>Ar</sub>), 8.09–8.06 (m, 2

**[H<sub>Ar</sub>], 7.98 (s, 1 H<sub>Ar</sub>, btz), 7.78 (t, 1 H<sub>Ar</sub>, bpy), 7.55 (d, 2 H<sub>Ar</sub>), 7.10 (d, <sup>3</sup>J = 7.3 Hz, 1 H<sub>Ar</sub>, bpy), 6.76 (d, <sup>3</sup>J = 7.4 Hz, 1 H<sub>Ar</sub>, bpy), 4.39–3.98 (“q”, J<sub>AB</sub> = 14.3 Hz, 2 H, OCH<sub>2</sub> btz<sub>A</sub>), 4.29–4.20 (“q”, J<sub>AB</sub> = 13.3 Hz, 2 H, OCH<sub>2</sub> bpy<sub>B</sub>), 3.99–3.90 (“q”, J<sub>AB</sub> = 8.2 Hz, 2 H, OCH<sub>2</sub>, bpy<sub>A</sub>), 2.48 (s, 3 H, CH<sub>3</sub>, btz<sub>B</sub>), 2.36 (s, 6 H, CH<sub>3</sub> bpy<sub>B</sub>, CH<sub>3</sub>, btz<sub>A</sub>), 2.15 (s, 3 H, CH<sub>3</sub>, bpy<sub>A</sub>) ppm. <sup>13</sup>C NMR (100 MHz, CD<sub>3</sub>CN, –30 °C; A and B could not be differentiated): δ = 166.6 (q, btz), 166.5 (q, btz), 164.4 (q, btz), 164.3 (q, btz), 156.9 (2 q, bpy), 154.4 (q, bpy), 153.9 (q, bpy), 150.8 (q, bpy), 150.5 (q, bpy), 150.4 (q, bpy), 149.9 (q, bpy), 147.4 (q, btz), 146.7 (q, btz), 146.0 (q, btz), 145.6 (q, btz), 138.2 (CH<sub>Ar</sub>, bpy), 138.0 (CH<sub>Ar</sub>, bpy), 137.8 (2 CH<sub>Ar</sub>, bpy), 125.6 (CH<sub>Ar</sub>, bpy), 125.2 (CH<sub>Ar</sub>, bpy), 122.9 (CH<sub>Ar</sub>, bpy), 121.3 (CH<sub>Ar</sub>, bpy), 120.5 (CH<sub>Ar</sub>, bpy), 119.9 (CH<sub>Ar</sub>, bpy), 119.0 (CH<sub>Ar</sub>, bpy), 118.6 (CH<sub>Ar</sub>, bpy), 116.0 (CH<sub>Ar</sub>, btz), 115.8 (CH<sub>Ar</sub>, btz), 115.5 (CH<sub>Ar</sub>, btz), 114.8 (CH<sub>Ar</sub>, btz), 70.6 (OCH<sub>2</sub>, bpy), 70.0 (OCH<sub>2</sub>, bpy), 65.5 (2 OCH<sub>2</sub>, btz), 24.3 (CH<sub>3</sub>, bpy), 23.9 (CH<sub>3</sub>, bpy), 17.8 (CH<sub>3</sub>, btz), 17.6 (CH<sub>3</sub>, btz) ppm. UV/Vis (CH<sub>3</sub>CN): λ<sub>max</sub> (ε<sub>max</sub>) = 260 (25380), 298 (14650), 448 (MLCT) (1698) nm. ESMS: *m/z* (%) = 1060.9 (45) [Cu<sub>2</sub>(10)<sub>2</sub>(PF<sub>6</sub><sup>–</sup>)<sub>2</sub>]<sup>+</sup>, 457.0 (100) [Cu<sub>2</sub>(7)<sub>2</sub>]<sup>2+</sup>/2. C<sub>40</sub>H<sub>36</sub>Cu<sub>2</sub>F<sub>12</sub>N<sub>8</sub>O<sub>2</sub>P<sub>2</sub>S<sub>4</sub> (1206.05): calcd. C 39.83, H 3.01, N 9.29; found C 39.89, H 3.10, N 9.35.**

**[Ag<sub>2</sub>(10)<sub>2</sub>][PF<sub>6</sub>]<sub>2</sub> (17):** AgPF<sub>6</sub> (64.2 mg, 0.25 mmol) was added to the ligand **10** (100 mg, 0.25 mmol) dissolved in anhydrous CH<sub>3</sub>CN (20 mL) under Ar. The mixture was stirred at room temperature and, after evaporation of the solvent, the solid residue was crystallised by slow diffusion of diethyl ether into an acetonitrile solution which gave white crystals. Yield 95%. <sup>1</sup>H NMR (400 MHz, CD<sub>3</sub>CN, 25 °C): δ = 8.14–8.04 (m, 3 H<sub>Ar</sub>, bpy), 7.88 (s, 1 H<sub>Ar</sub>, btz), 7.82 (t, 1 H<sub>Ar</sub>, bpy, s, 1 H<sub>Ar</sub>, btz), 7.54 (d, <sup>3</sup>J = 7.6 Hz, 1 H<sub>Ar</sub>, bpy), 7.16 (d, <sup>3</sup>J = 6.8 Hz, 1 H<sub>Ar</sub>, bpy), 4.50 (s, 2 H, OCH<sub>2</sub>, btz), 4.34 (s, 2 H, OCH<sub>2</sub>, bpy), 2.53 (s, 3 H, CH<sub>3</sub>, btz), 2.49 (s, 3 H, CH<sub>3</sub>, bpy) ppm. <sup>13</sup>C NMR (100 MHz, CD<sub>3</sub>CN, 25 °C): δ = 169.1 (q, btz), 167.7 (q, btz), 158.9 (q, bpy), 156.2 (q, bpy), 151.5 (q, bpy), 150.9 (q, bpy), 147.6 (q, btz), 146.8 (q, btz), 140.0 (CH<sub>Ar</sub>, bpy), 139.9 (CH<sub>Ar</sub>, bpy), 125.9 (CH<sub>Ar</sub>, bpy), 123.8 (CH<sub>Ar</sub>, bpy), 122.1 (CH<sub>Ar</sub>, bpy), 120.5 (CH<sub>Ar</sub>, bpy), 117.0 (CH<sub>Ar</sub>, btz), 116.9 (CH<sub>Ar</sub>, btz), 73.4 (OCH<sub>2</sub>, bpy), 68.1 (OCH<sub>2</sub>, btz), 26.5 (CH<sub>3</sub>, bpy), 19.2 (CH<sub>3</sub>, btz) ppm. UV/Vis (CH<sub>3</sub>CN): λ<sub>max</sub> (ε<sub>max</sub>) = 295 (14000) nm. ESMS: *m/z* (%) = 503.2 (20) [Ag<sub>2</sub>(10)<sub>2</sub>]<sup>2+</sup>/2. C<sub>40</sub>H<sub>36</sub>Ag<sub>2</sub>F<sub>12</sub>N<sub>8</sub>O<sub>2</sub>P<sub>2</sub>S<sub>4</sub>·2H<sub>2</sub>O (1330.73): calcd. C 36.10, H 3.03, N 8.42; found C 35.75, H 2.74, N 8.53.

**[Zn<sub>2</sub>(10)<sub>2</sub>][OTf]<sub>4</sub> (18):** Zn(OTf)<sub>2</sub> (28.2 mg, 0.076 mmol) was added to the ligand **10** (30 mg, 0.076 mmol) dissolved in CH<sub>3</sub>OH (10 mL) under Ar. The solution was stirred at room temperature for 1 h and the solvent was evaporated giving a yellow powder. Yield 98%. Mixture of diastereoisomers A/B (18:82) in solution. <sup>1</sup>H NMR (400 MHz, CD<sub>3</sub>OD, 25 °C): δ = 8.71 (d, <sup>3</sup>J = 8.2 Hz, 1 H<sub>Ar</sub>, bpy<sub>B</sub>), 8.52 (d, <sup>3</sup>J = 8.0 Hz, 1 H<sub>Ar</sub>, bpy<sub>B</sub>), 8.45 (t, <sup>3</sup>J = 8.0 Hz, 1 H<sub>Ar</sub>, bpy<sub>B</sub>), 8.15 (t, <sup>3</sup>J = 8.0 Hz, 1 H<sub>Ar</sub>, bpy<sub>B</sub>), 7.89 (d, <sup>3</sup>J = 8.2 Hz, 1 H<sub>Ar</sub>, bpy<sub>B</sub>), 7.67 (s, 1 H<sub>Ar</sub>, btz<sub>B</sub>), 7.57 (s, 1 H<sub>Ar</sub>, btz<sub>B</sub>), 7.51 (d, <sup>3</sup>J = 7.8 Hz, 1 H<sub>Ar</sub>, bpy<sub>B</sub>), 5.51–5.40 (“q”, AB, J<sub>AB</sub> = 15.8 Hz, 2 H, OCH<sub>2</sub>, btz<sub>B</sub>), 5.13 (s, 4 H, CH<sub>2</sub>OCH<sub>2</sub>, A), 4.53–4.46 (“q”, AB, J<sub>AB</sub> = 14.7 Hz, 2 H, OCH<sub>2</sub>, bpy<sub>B</sub>), 2.78 (s, 3 H, CH<sub>3</sub>, btz<sub>B</sub>), 2.66 (s, 3 H, CH<sub>3</sub>, btz<sub>A</sub>), 2.14 (s, 3 H, CH<sub>3</sub>, bpy<sub>A</sub>), 1.91 (s, 3 H, CH<sub>3</sub>, bpy<sub>B</sub>) ppm. <sup>13</sup>C NMR (100 MHz, CD<sub>3</sub>OD, 25 °C): δ = 159.8, 159.6, 149.6, 148.7, 148.0 (4 q, btz, 4 q, bpy), 143.8, 143.7, 143.4, 142.9, 142.7 (4 CH<sub>Ar</sub>, bpy), 129.1, 125.5, 123.3, 122.3, 122.6, 122.3, 121.4, 119.2, 118.1, 117.0, 116.8, 116.2, 116.0 (8 CH<sub>Ar</sub>, bpy, 4 CH<sub>Ar</sub>, btz), 69.9, 69.7, 68.9, 68.1 (2 OCH<sub>2</sub>, btz, 2 OCH<sub>2</sub>, bpy), 23.1, 22.2 (2 CH<sub>3</sub>, bpy), 17.9, 16.5 (2 CH<sub>3</sub>, btz) ppm. UV/Vis (CH<sub>3</sub>OH): λ = 248 nm (24175), 303 (13403) nm. ESIMS: *m/z* (%) = 1363.0 (9)

[Zn<sub>2</sub>(10)<sub>2</sub>(OTf)<sub>3</sub>]<sup>+</sup>, 1001.0 (22) [Zn(10)<sub>2</sub>(OTf)]<sup>+</sup>, 607.0 (100) [Zn<sub>2</sub>(10)<sub>2</sub>(OTf)<sub>2</sub>]<sup>2+</sup>/2, 229.0 (45) [Zn<sub>2</sub>(10)<sub>2</sub>]<sup>4+</sup>/4.

**[Cu<sub>2</sub>(11)<sub>2</sub>][PF<sub>6</sub>]<sub>2</sub> (19):** [Cu(CH<sub>3</sub>CN)<sub>4</sub>][PF<sub>6</sub>]<sub>2</sub> (145.6 mg, 0.39 mmol) was added to the ligand **11** (150 mg, 0.39 mmol) dissolved in anhydrous CH<sub>3</sub>CN (30 mL) under Ar. The mixture was stirred at room temperature, which instantly gave a deep-red solution. After evaporation of the solvent, the solid residue was recrystallised by slow diffusion of diethyl ether into an acetonitrile solution which gave deep-red crystals. Yield 94%. Mixture of diastereoisomers A/B (55:45) in solution. <sup>1</sup>H NMR (400 MHz, CD<sub>3</sub>CN, –30 °C): δ = 9.25 (d, <sup>3</sup>J = 5.0 Hz, 1 H, bpm<sub>A</sub>), 9.22 (d, <sup>3</sup>J = 5.2 Hz, 1 H, bpm<sub>B</sub>), 9.05 (d, <sup>3</sup>J = 5.0 Hz, 1 H, bpm<sub>B</sub>), 8.90 (d, <sup>3</sup>J = 5.1 Hz, 1 H, bpm<sub>A</sub>), 8.40–8.30 (m, 7 H, A and B), 8.25 (d, <sup>3</sup>J = 8.0 Hz, 1 H, bpy<sub>B</sub>), 8.16–8.08 (m, 2 H, A and B), 8.00 (t, <sup>3</sup>J = 7.6 Hz, 1 H, bpy<sub>A</sub>), 7.87 (t, <sup>3</sup>J = 7.8 Hz, 1 H, bpy<sub>B</sub>), 7.57 (d, <sup>3</sup>J = 7.4 Hz, 1 H, bpy<sub>B</sub>), 7.53 (d, <sup>3</sup>J = 7.6 Hz, 1 H, bpy<sub>A</sub>), 6.97 (d, <sup>3</sup>J = 7.4 Hz, 1 H, bpy<sub>A</sub>), 6.87 (d, <sup>3</sup>J = 7.6 Hz, 1 H, bpy<sub>B</sub>), 4.15–3.90 (m, 4 H, OCH<sub>2</sub>, bpm<sub>A</sub>, OCH<sub>2</sub>, bpm<sub>B</sub>), 4.15–3.80 (“q”, AB, J<sub>AB</sub> = 13.5 Hz, 2 H, OCH<sub>2</sub>, bpy<sub>A</sub>), 4.15–3.62 (“q”, AB, J<sub>AB</sub> = 13.2 Hz, 2 H, OCH<sub>2</sub>, bpy<sub>B</sub>), 2.49 (s, 3 H, CH<sub>3</sub>, bpm<sub>A</sub>), 2.36 (s, 3 H, CH<sub>3</sub>, bpm<sub>B</sub>), 2.18 (s, 3 H, CH<sub>3</sub>, bpy<sub>B</sub>), 2.06 (s, 3 H, CH<sub>3</sub>, bpy<sub>A</sub>) ppm. <sup>13</sup>C NMR (100 MHz, CD<sub>3</sub>CN, –30 °C): δ = 167.0, 166.7 (q, bpm<sub>A</sub>, q, bpm<sub>B</sub>), 163.9, 163.8 (q, bpm<sub>A</sub>, q, bpm<sub>B</sub>), 159.6, 159.2, 159.0, 158.7 (2 CH, bpm<sub>A</sub>, 2 CH, bpm<sub>B</sub>), 157.3, 157.0, 156.7, 156.5 (2 q, bpm<sub>A</sub>, 2 q, bpm<sub>B</sub>), 155.5, 155.2, 154.4, 154.3 (2 q, bpy<sub>A</sub>, 2 q, bpy<sub>B</sub>), 150.9, 150.8, 150.1, 149.8 (2 q, bpy<sub>A</sub>, 2 q, bpy<sub>B</sub>), 138.8, 138.4, 138.3, 138.0 (2 CH, bpy<sub>A</sub>, 2 CH, bpy<sub>B</sub>), 125.8, 125.7 (CH, bpy<sub>A</sub>, CH, bpy<sub>B</sub>), 123.0, 122.9 (CH, bpy<sub>A</sub>, CH, bpy<sub>B</sub>), 120.8, 120.7 (CH, bpy<sub>A</sub>, CH, bpy<sub>B</sub>), 119.2, 119.0 (CH, bpy<sub>A</sub>, CH, bpy<sub>B</sub>), 117.6, 117.5 (CH, bpm<sub>A</sub>, CH, bpm<sub>B</sub>), 116.0, 115.8 (CH, bpm<sub>A</sub>, CH, bpm<sub>B</sub>), 71.6, 71.2 (OCH<sub>2</sub>, bpm<sub>A</sub>, OCH<sub>2</sub>, bpm<sub>B</sub>), OCH<sub>2</sub>, bpy<sub>A</sub>, OCH<sub>2</sub>, bpy<sub>B</sub>), 26.0, 25.6, 24.4, 23.9 (CH<sub>3</sub>, bpm<sub>A</sub>, CH<sub>3</sub>, bpm<sub>B</sub>, CH<sub>3</sub>, bpy<sub>A</sub>, CH<sub>3</sub>, bpy<sub>B</sub>) ppm. UV/Vis (CH<sub>3</sub>CN): λ<sub>max</sub> (ε) = 279 (20602), 287 (20838), 450 (MLCT) (1759) nm. ESIMS: *m/z* (%) = 447.3 (8) [Cu<sub>2</sub>(11)<sub>2</sub>]<sup>2+</sup>/2. C<sub>44</sub>H<sub>40</sub>Cu<sub>2</sub>F<sub>12</sub>N<sub>12</sub>O<sub>2</sub>P<sub>2</sub>·0.25CH<sub>2</sub>Cl<sub>2</sub> (1207.12): calcd. C 44.03, H 3.38, N 13.92; found C 43.84, H 3.42, N 13.99.

**[Ag<sub>2</sub>(11)<sub>2</sub>][PF<sub>6</sub>]<sub>2</sub> (20):** AgPF<sub>6</sub> (65.84 mg, 0.26 mmol) was added to the ligand **11** (100 mg, 0.26 mol) dissolved in anhydrous CH<sub>3</sub>CN (20 mL) under Ar. The mixture was stirred at room temperature and after evaporation of the solvent, the solid residue was recrystallised by slow diffusion of diethyl ether into an acetonitrile solution which gave white crystals. Yield 92%. <sup>1</sup>H NMR (400 MHz, CD<sub>3</sub>CN, 25 °C): δ = 9.06 (d, <sup>3</sup>J = 5.4 Hz, 1 H, bpm), 8.95 (d, <sup>3</sup>J = 5.3 Hz, 1 H, bpm), 8.21 (d, <sup>3</sup>J = 5.2 Hz, 1 H, bpm), 8.18 (d, <sup>3</sup>J = 5.3 Hz, 1 H, bpm), 8.06 (d, <sup>3</sup>J = 6.5 Hz, 1 H, bpy), 8.03 (t, <sup>3</sup>J = 8.0 Hz, 1 H, bpy), 7.95 (d, <sup>3</sup>J = 8.0 Hz, 1 H, bpy), 7.62 (t, <sup>3</sup>J = 7.6 Hz, 1 H, bpy), 7.57 (d, <sup>3</sup>J = 7.4 Hz, 1 H, bpy), 6.93 (d, <sup>3</sup>J = 7.4 Hz, 1 H, bpy), 4.45 (s, 4 H, CH<sub>2</sub>OCH<sub>2</sub>), 2.56 (s, 3 H, CH<sub>3</sub>, bpm), 2.35 (s, 3 H, CH<sub>3</sub>, bpy) ppm. <sup>13</sup>C NMR (100 MHz, CD<sub>3</sub>CN, 25 °C): δ = 169.2 (q, bpm), 165.8 (q, bpm), 160.8 (CH, bpm), 160.9 (CH, bpm), 158.9 (q, bpm), 158.0 (q, bpm), 156.9 (q, bpy), 155.3 (q, bpy), 151.6 (q, bpy), 150.4 (q, bpy), 139.9 (CH, bpm), 139.8 (CH, bpm), 126.2 (CH, bpm), 124.6 (CH, bpm), 122.3 (CH, bpm), 120.6 (CH, bpm), 118.9 (CH, bpm), 117.1 (CH, bpm), 73.7 (OCH<sub>2</sub>, bpm), 71.9 (OCH<sub>2</sub>, bpm), 26.4 (CH<sub>3</sub>, bpm), 26.3 (CH<sub>3</sub>, bpm) ppm. UV/Vis (CH<sub>3</sub>CN): λ<sub>max</sub> (ε) = 288 (21700) nm. ESIMS: *m/z* (%) = 491.3 (24) [Ag<sub>2</sub>(11)<sub>2</sub>]<sup>2+</sup>/2. C<sub>44</sub>H<sub>40</sub>Ag<sub>2</sub>F<sub>12</sub>N<sub>12</sub>O<sub>2</sub>P<sub>2</sub>·CH<sub>2</sub>Cl<sub>2</sub>·H<sub>2</sub>O (11377.49): calcd. C 39.24, H 3.22, N 12.20; found C 39.15, H 3.06, N 12.38.

**[Zn<sub>2</sub>(11)<sub>2</sub>][OTf]<sub>4</sub> (21):** Zn(OTf)<sub>2</sub> (89 mg, 0.24 mmol) was added to the ligand **11** (92 mg, 0.24 mmol) dissolved in CH<sub>3</sub>OH (30 mL) un-

der Ar. The mixture was stirred at room temperature for 1 h. After evaporation of the solvent, the solid residue was recrystallised by slow evaporation of a methanolic solution which gave white crystals. Yield 95%. Mixture of diastereoisomers A/B (83:17) in solution.  $^1\text{H}$  NMR (400 MHz,  $\text{CD}_3\text{OD}$ , 25 °C):  $\delta$  = 9.32 (d,  $^3J$  = 5.7 Hz, 1 H, bpm<sub>A</sub>), 9.02 (d,  $^3J$  = 5.2 Hz, 1 H, bpm<sub>A</sub>), 8.89 (d,  $^3J$  = 5.2 Hz, 1 H, bpm<sub>B</sub>), 8.84 (d,  $^3J$  = 5.7 Hz, 1 H, bpm<sub>A</sub>), 8.72–8.61 (2 H, B), 8.71 (d,  $^3J$  = 7.1 Hz, 1 H, bpy<sub>A</sub>), 8.63 (d,  $^3J$  = 8.0 Hz, 1 H, bpy<sub>A</sub>), 8.47–8.33 (3 H, B), 8.45 (t,  $^3J$  = 7.8 Hz, 1 H, bpy<sub>A</sub>), 8.41 (d,  $^3J$  = 5.2 Hz, 1 H, bpm<sub>A</sub>), 8.36 (t,  $^3J$  = 8.0 Hz, 1 H, bpy<sub>A</sub>), 8.22 (d,  $^3J$  = 5.0 Hz, 1 H, bpm<sub>B</sub>), 8.05–8.00 (m, 2 H, B), 7.93–7.89 (m, 2 H, bpy<sub>A</sub>, 1 H, B), 7.37 (d,  $^3J$  = 7.8 Hz, 1 H, bpy<sub>B</sub>), 5.69–5.40 (“q”, AB,  $J_{\text{AB}}$  = 15.4 Hz, 2 H, OCH<sub>2</sub>, bpm<sub>B</sub>), 5.56 (s, 2 H, OCH<sub>2</sub>, bpm<sub>A</sub>), 5.50 (s, 2 H, OCH<sub>2</sub>, bpy<sub>A</sub>), 4.61–4.23 (“q”, AB,  $J_{\text{AB}}$  = 15.8 Hz, 2 H, OCH<sub>2</sub>, bpy<sub>B</sub>), 3.12 (s, 3 H, CH<sub>3</sub>, bpy<sub>A</sub>), 2.87 (s, CH<sub>3</sub>, bpm<sub>A</sub>), 2.81 (s, CH<sub>3</sub>, bpy<sub>B</sub>), 1.89 (s, CH<sub>3</sub>, bpm<sub>B</sub>) ppm.  $^{13}\text{C}$  NMR (100 MHz,  $\text{CD}_3\text{OD}$ , 25 °C):  $\delta$  = 169.0 (q, bpm<sub>A</sub>), 168.7 (q, bpm<sub>B</sub>), 165.7 (q, bpm<sub>B</sub>), 164.8 (q, bpm<sub>A</sub>), 164.7 (q, bpm<sub>A</sub>), 161.4 (q, bpm<sub>B</sub>), 160.8 (q, bpm<sub>B</sub>), 159.8 (q, bpy<sub>B</sub>), 159.6 (CH, bpm<sub>A</sub>), 159.5 (CH, bpm<sub>B</sub>, q, bpm<sub>A</sub>), 159.1 (CH, bpm<sub>B</sub>), 158.7 (q, bpy<sub>A</sub>), 157.7 (CH, bpm<sub>A</sub>), 157.0 (q, bpy<sub>B</sub>), 154.4 (q, bpy<sub>A</sub>), 148.8 (q, bpy<sub>A</sub>), 148.5 (q, bpy<sub>B</sub>), 148.4 (q, bpy<sub>A</sub>), 148.0 (q, bpy<sub>B</sub>), 143.6 (CH, bpy<sub>B</sub>), 143.0 (CH, bpy<sub>A</sub>), 142.7 (CH, bpy<sub>B</sub>), 142.6 (CH, bpy<sub>A</sub>), 128.8 (CH, bpy<sub>B</sub>), 128.2 (CH, bpy<sub>A</sub>), 125.5 (CH, bpy<sub>B</sub>), 124.2 (CH, bpy<sub>A</sub>), 122.8 (CH, bpy<sub>B</sub>), 122.0 (CH, bpy<sub>A</sub>), 121.0 (CH, bpy<sub>B</sub>), 120.9 (CH, bpy<sub>A</sub>), 119.28 (CH, bpm<sub>A</sub>), 116.8 (CH, bpm<sub>B</sub>), 115.8 (CH, bpm<sub>A</sub>), 115.1 (CH, bpm<sub>B</sub>), 72.4 (OCH<sub>2</sub>, bpm<sub>B</sub>), 70.5 (OCH<sub>2</sub>, bpm<sub>A</sub>), 70.3 (OCH<sub>2</sub>, bpy<sub>B</sub>), 68.8 (OCH<sub>2</sub>, bpy<sub>A</sub>), 25.0, 24.7, 22.3 (CH<sub>3</sub>, bpm<sub>A</sub>, CH<sub>3</sub>, bpm<sub>B</sub>, CH<sub>3</sub>, bpy<sub>A</sub>, CH<sub>3</sub>, bpy<sub>B</sub>) ppm. UV/Vis ( $\text{CH}_3\text{CN}$ ):  $\lambda_{\text{max}}$  ( $\epsilon$ ) = 298 (21000), 305 (18971), 316 (17651) nm. ESIMS:  $m/z$  (%) = 1342.1 (4)  $[\text{Zn}_2(\mathbf{11})_2(\text{OTf})_3]^+$ , 981.3 (42)  $[\text{Zn}(\mathbf{11})_2(\text{OTf})]^+$ , 597.2 (10)  $[\text{Zn}_2(\mathbf{11})_2(\text{OTf})_2]^{2+}/2$ , 416.3 (22)  $[\text{Zn}(\mathbf{11})_2]^{2+}/2$ , 224.3 (100)  $[\text{Zn}_2(\mathbf{11})_2]^{4+}/4$ .

[Ag<sub>2</sub>(**12**)<sub>2</sub>(PF<sub>6</sub>)<sub>2</sub>] (**22**): Data see ref.<sup>[5]</sup>

[Zn<sub>2</sub>(**12**)<sub>2</sub>][OTf]<sub>4</sub> (**23**): Zn(OTf)<sub>2</sub> (89 mg, 0.24 mmol) was added to the ligand **12** (92 mg, 0.24 mmol) dissolved in CH<sub>3</sub>OH (30 mL) under Ar. The mixture was stirred at room temperature for 1 h and the solvent was evaporated. Yield 98%.  $^1\text{H}$  NMR (400 MHz,  $\text{CD}_3\text{OD}$ , 25 °C):  $\delta$  = 9.31 (s, 1 H, bpz), 8.92 (s, 1 H, bpz), 8.62 (d,  $^3J$  = 7.8 Hz, 1 H, bpy), 8.62 (s, 1 H, bpz), 8.46 (t,  $^3J$  = 8.0 Hz, 1 H, bpy), 8.40 (d,  $^3J$  = 8.0 Hz, 1 H, bpy), 8.13 (s, 1 H, bpz), 8.06 (t,  $^3J$  = 7.8 Hz, 1 H, bpy), 7.95 (d,  $^3J$  = 7.8 Hz, 1 H, bpy), 7.35 (d,  $^3J$  = 7.8 Hz, 1 H, bpy), 5.60–5.45 (“q”, AB,  $J_{\text{AB}}$  = 15.4 Hz, 2 H, OCH<sub>2</sub>, bpy), 4.63–4.44 (“q”, AB,  $J_{\text{AB}}$  = 14.7 Hz, 2 H, OCH<sub>2</sub>, bpz), 2.70 (s, 3 H, CH<sub>3</sub>, bpz), 1.82 (s, 3 H, CH<sub>3</sub>, bpy) ppm.  $^{13}\text{C}$  NMR (100 MHz,  $\text{CD}_3\text{OD}$ , 25 °C):  $\delta$  = 159.7 (q, bpy), 156.7 (q, bpy), 154.6 (q, bpy), 150.5 (q, bpy), 149.0 (q, bpz), 148.6 (q, bpz), 147.9 (q, bpz), 147.8 (q, bpz), 145.5 (CH, bpz), 143.9 (CH, bpy), 143.4 (CH, bpz), 142.9 (CH, bpy), 142.6 (CH, bpz), 139.5 (CH, bpz), 129.0 (CH, bpy), 125.6 (CH, bpy), 123.1 (CH, bpy), 121.2 (CH, bpy), 71.2 (OCH<sub>2</sub>, bpz), 70.5 (OCH<sub>2</sub>, bpy), 22.2 (CH<sub>3</sub>, bpy), 20.7 (CH<sub>3</sub>, bpz) ppm. UV/Vis ( $\text{CH}_3\text{OH}$ ):  $\lambda_{\text{max}}$  ( $\epsilon$ ) = 233 (16728), 296 (28491) nm. ESIMS:  $m/z$  (%) = 1343.3 (5)  $[\text{Zn}_2(\mathbf{12})_2(\text{OTf})_3]^+$ , 981.4 (64)  $[\text{Zn}(\mathbf{12})_2(\text{OTf})]^+$ , 597.2 (13)  $[\text{Zn}_2(\mathbf{12})_2(\text{OTf})_2]^{2+}/2$ , 416.3 (95)  $[\text{Zn}(\mathbf{12})_2]^{2+}$ , 224.2 (98)  $[\text{Zn}_2(\mathbf{12})_2]^{4+}/2$ .

**X-ray Crystallographic Study:** The crystal structures of  $[\text{Ag}(\text{C}_{22}\text{H}_{20}\text{N}_6\text{O})_2][\text{PF}_6]_2[\text{CH}_3\text{N}]$  (**20**) [ $\rho_{\text{calcd.}}$  = 1.70  $\text{Mg}\cdot\text{m}^{-3}$ ,  $\mu$  (Mo- $K_{\alpha}$ ) = 0.924  $\text{mm}^{-1}$ ] and  $[\text{Ag}(\text{C}_{22}\text{H}_{20}\text{N}_6\text{O})_2][\text{PF}_6]_2$  (**22**) [ $\rho_{\text{calcd.}}$  = 1.74  $\text{Mg}\cdot\text{m}^{-3}$ ,  $\mu$  (Mo- $K_{\alpha}$ ) = 0.926  $\text{mm}^{-1}$ ] were determined from single-crystal X-ray diffraction experiments using Mo- $K_{\alpha}$  X-ray radiation ( $\lambda$  = 0.71073 Å) with a Siemens Smart CCD diffractometer. Both

compounds crystallized in the triclinic  $P\bar{1}$  space group,  $Z$  = 2. The cell parameters for complex **20** are  $a$  = 13.705(2),  $b$  = 14.010(2),  $c$  = 14.277(3) Å,  $\alpha$  = 90.47(1),  $\beta$  = 96.31(1),  $\gamma$  = 109.83(1)°,  $V$  = 2560.1(2) Å<sup>3</sup>. The cell parameters for complex **22** are  $a$  = 12.019 (1),  $b$  = 15.153(2),  $c$  = 15.186(2) Å,  $\alpha$  = 75.08(1),  $\beta$  = 70.89(1),  $\gamma$  = 71.13(1)°,  $V$  = 2437.0(1) Å<sup>3</sup>. 11193 and 10720 reflections were collected up to  $\theta_{\text{max.}}$  = 23.4° for complexes **20** and **22**, respectively. The structures were solved by semi-invariant methods using the SIR92 module in the WINGX package.<sup>[21]</sup> The structures were refined by the full-matrix least-squares method based on  $F^2$  using the SHELX97<sup>[23]</sup> program. Thermal displacements of non-hydrogen atoms were refined anisotropically. Hydrogen atoms were included at their idealized positions but not refined. For complex **20**, the final statistical factors were found equal to  $R1(\text{all observed data})$  = 0.058,  $wR2$  = 0.130 for 7349 data and 695 parameters,  $R1[F^2 > 2\sigma(I)]$  = 0.050 for 6374 data with  $F^2 > 2\sigma(I)$ . The final residual densities in the unit cell were +0.81 and -0.58 e·Å<sup>-3</sup>. For complex **22**, the final statistical factors were found equal to  $R1(\text{all observed data})$  = 0.095,  $wR2$  = 0.170 for 7009 data and 667 parameters,  $R1[F^2 > 2\sigma(I)]$  = 0.073 for 5541 data with  $F^2 > 2\sigma(I)$ . The final residual densities in the unit cell were +0.92 and -0.64 e·Å<sup>-3</sup>. The crystal structures of  $[\text{Cu}_2(\text{C}_{20}\text{H}_{18}\text{N}_4\text{O}_5)_2(\text{C}_3\text{H}_6\text{O})][\text{PF}_6]_2$  (**13**) [ $\rho_{\text{calcd.}}$  = 1.62  $\text{g}\cdot\text{cm}^{-3}$ ,  $\mu$  (Mo- $K_{\alpha}$ ) = 1.13  $\text{mm}^{-1}$ ] and  $[\text{Cu}(\text{C}_{20}\text{H}_{18}\text{N}_4\text{O}_5)_2][\text{PF}_6]_2$  (**16**) [ $\rho_{\text{calcd.}}$  = 1.55  $\text{g}\cdot\text{cm}^{-3}$ ,  $\mu$  (Mo- $K_{\alpha}$ ) = 1.13  $\text{mm}^{-1}$ ], were determined from single-crystal X-ray diffraction experiments performed with an Enraf-Nonius CAD-4F diffractometer at room temperature. Large crystal samples (**13**: red, 0.6 × 0.5 × 0.3 mm; **16**: orange, 0.9 × 0.6 × 0.5 mm) were chosen for the experiments using Mo- $K_{\alpha}$  X-ray radiation ( $\lambda$  = 0.71073 Å). Both compounds crystallized in the triclinic  $P\bar{1}$  space group,  $Z$  = 2 (**13**) and 4 (**16**). The unit cell parameters were obtained by least-squares fit to setting angles of 25 reflections in the range 8° < 2θ < 36° (**13**) and 12° < 2θ < 40° (**16**). The cell parameters are  $a$  = 13.336(5),  $b$  = 13.437(4),  $c$  = 15.874(5) Å,  $\alpha$  = 90.63(2),  $\beta$  = 98.82(3),  $\gamma$  = 111.96(2)°,  $V$  = 2599(2) Å<sup>3</sup> (**13**) and  $a$  = 12.682(5),  $b$  = 19.688(5),  $c$  = 21.624(5) Å,  $\alpha$  = 100.810(5),  $\beta$  = 97.364(5),  $\gamma$  = 99.628(5)°,  $V$  = 5157(3) Å<sup>3</sup> (**16**). The  $\omega$ -2θ scan mode was used to record the diffracted intensities. Three standard reflections were monitored every 2 h in order to control the intensity decay, which did not occur significantly. 8485 and 25719 reflections were collected up to  $2\theta_{\text{max.}}$  = 55.3 (**13**) and 59.9° (**16**). Lorentz-polarisation corrections and data reduction were performed using the WINGX package<sup>[26]</sup> for CAD4-collected intensities. The structures were solved by direct methods using the SIR92 program<sup>[22]</sup> and refined by the full-matrix least-squares method based on  $F^2$  using the SHELX97<sup>[23]</sup> program. Thermal displacements of non-hydrogen atoms were refined anisotropically. Hydrogen atoms were included at their idealized positions. In the last cycles of refinement, the best results were obtained with empirical absorption corrections using the XABS2 (**13**) and DIFABS (**16**) programs in the WINGX package.<sup>[21]</sup> For the complex **13**, the final statistical factors were found equal to  $R1(\text{all data})$  = 0.261,  $wR2$  = 0.498 for 8485 data and 668 parameters,  $R1[F^2 > 2\sigma(I)]$  = 0.183 for 3790 data with  $F^2 > 2\sigma(I)$  and the final residual densities in the unit cell were +1.14 and -1.51 e·Å<sup>-3</sup>. For the complex **16**, the results were  $R1(\text{all data})$  = 0.258,  $wR2$  = 0.419 for 23950 data and 1231 parameters,  $R1[F^2 > 2\sigma(I)]$  = 0.122 for 9291 data with  $F^2 > 2\sigma(I)$  and the final residual densities in the unit cell were +1.95 and -0.86 e·Å<sup>-3</sup>. CCDC-205779 (**20**), -205780 (**22**), -201694 (**13**) and -201695 (**16**) contain the supplementary crystallographic data for this paper. These data can be obtained free of charge at [www.ccdc.cam.ac.uk/conts/retrieving.html](http://www.ccdc.cam.ac.uk/conts/retrieving.html) [or from the Cambridge Crystallographic Data Centre, 12 Union Road, Cambridge CB2 1EZ, UK; Fax: (internat.) + 44-1223/336-033; E-mail: [deposit@ccdc.cam.ac.uk](mailto:deposit@ccdc.cam.ac.uk)].

## Acknowledgments

We are grateful to the CNRS and the MESR for financial support. We also thank Mr. J. M. Ziegler for recording ES mass spectra, Mrs. E. Eppiger and P. Mutzenhardt for recording NMR spectra, and Mrs N. Marshall for correcting the manuscript.

- [1] J.-M. Lehn, *Supramolecular Chemistry*, Wiley-VCH, Weinheim, 1995.
- [2] Reviews dealing with helicates: [2a] E. C. Constable, *Tetrahedron* **1992**, *48*, 113–159. [2b] C. Piguet, G. Bernardinelli, G. Hopfgartner, *Chem. Rev.* **1997**, *97*, 2005–2062. [2c] M. Albrecht, *Chem. Eur. J.* **2000**, *6*, 3485–3489. [2d] M. Albrecht, M. Schneider, *Eur. J. Inorg. Chem.* **2002**, 1301–1306. [2e] A. Lützen, M. Hapke, J. Griep-Raming, D. Haase, W. Saak, *Angew. Chem. Int. Ed.* **2002**, *41*, 2086–2089, *Angew. Chem.* **2002**, *114*, 2190–2194. Reviews dealing with heterodimetallic helicates: [2f] M. Albrecht, *Chem. Rev.* **2001**, *101*, 3457–3497. [2g] E. C. Constable, J. V. Walker, *J. Chem. Soc., Chem. Commun.* **1992**, 884–885. [2h] E. C. Constable, A. J. Edwards, R. Raithby, J. V. Walker, *Angew. Chem. Int. Ed. Engl.* **1993**, *32*, 1465–1466. [2i] C. Piguet, J.-C. G. Bünzli, *Chem. Soc. Rev.* **1999**, *28*, 347–358.
- [3] C. R. Rice, S. Wörl, J. C. Jeffery, R. L. Paul, M. D. Ward, *J. Chem. Soc., Chem. Commun.* **2000**, 1529–1530.
- [4] M. Albrecht, R. Fröhlich, *J. Am. Chem. Soc.* **1997**, *119*, 1656–1661.
- [5] J. Mathieu, A. Marsura, N. Bouhmaida, N. Ghermani, *Eur. J. Inorg. Chem.* **2002**, 2433–2437.
- [6] K. Roussel, A. Cartier, A. Marsura, *Chem. Phys. Lett.* **2003**, *367*, 463–467.
- [7] M. Wagner, P. Engrand, J.-B. Regnouf de Vains, A. Marsura, *Tetrahedron Lett.* **2001**, *42*, 5207–5209.
- [8] L. C. Hensley, N. Y. Binghampton (General Aniline & Film Corp.), US Patent 2,553,502, **1951**, [*Chem. Abstr.* **1958**, *54*, 18378a].
- [9] [9a] F. Effenberger, *Chem. Ber.* **1965**, *98*, 2260–2265. [9b] C. Janiak, L. Uhelin, H. Wu, P. Klüfers, H. G. Piotrowski, T. Scharmann, *J. Chem. Soc., Dalton Trans.* **1999**, 3121–3131.
- [10] G. R. Newkome, W. E. Puckett, G. E. Kiefer, V. K. Gupta, Y. Xia, M. Coreil, M. A. Hackney, *J. Org. Chem.* **1982**, *47*, 4116–4120.
- [11] log $\beta$  values were calculated using the SPECFIT<sup>®</sup> program version 3.0 (Ed.: R. A. Binstead), Spectrum Software Associates, **1993–2001**.
- [12] G. Hopfgartner, C. Piguet, J. D. Henion, A. F. Williams, *Helv. Chim. Acta* **1993**, *32*, 1759–1766.
- [13] See Supporting Information; see also the footnote on the first page of this article.
- [14] J.-M. Lehn, A. Rigault, *Angew. Chem. Int. Ed. Engl.* **1988**, *27*, 1095–1097; *Angew. Chem.* **1988**, *100*, 1121–1122.
- [15] C. Provent, E. Rivara-Minten, S. Hewage, G. Brunner, A. F. Williams, *Chem. Eur. J.* **1999**, *5*, 3487–3494.
- [16] S. Rüttimann, C. Piguet, G. Bernardinelli, B. Bocquet, A. F. Williams, *J. Am. Chem. Soc.* **1992**, *114*, 4230–4237.
- [17] [17a] A. Bilyk, M. M. Harding, *J. Chem. Soc., Dalton Trans.* **1994**, 77–82. [17b] A. Bilyk, M. M. Harding, P. Turner, T. W. Hambley, *J. Chem. Soc., Dalton Trans.* **1994**, 2783–2790.
- [18] M. Greenwald, D. Wessely, E. Katz, L. Willner, Y. Cohen, *J. Org. Chem.* **2000**, *65*, 1050–1058.
- [19] M. N. Burnett, C. K. Johnson, ORTEP-III report ORNL-6895, **1996**, Oak Ridge International Laboratory, Tennessee, USA.
- [20] MOLEKEL: An Interactive Molecular Graphic Tool: S. Portmann, H. P. Lüthi, *CHIMIA* **2000**, *54*, 766–770.
- [21] L. J. Farrugia, *J. Appl. Crystallogr.* **1999**, *32*, 837–838.
- [22] A. Altomare, G. Casciarano, C. Giacovazzo, A. Guagliardi, *J. Appl. Crystallogr.* **1993**, *26*, 343–350.
- [23] G. M. Sheldrick, *SHELXL-97 and SHELXS-97: Program for the Refinement of Crystal Structures*, University of Göttingen, Germany, **1997**.
- [24] F. Bodar-Houillon, Y. Elissami, A. Marsura, N. E. Ghermani, E. Espinosa, N. Bouhmaida, A. Thalal, *Eur. J. Org. Chem.* **1999**, 1427–1440.
- [25] F. Bodar-Houillon, T. Humbert, A. Marsura, *Inorg. Chem.* **1995**, *34*, 5205–5209.
- [26] N. E. Ghermani, N. Bouhmaida, C. Lecomte, A. L. Papet, A. Marsura, *J. Phys. Chem.* **1994**, *98*, 6287–6292.

Received December 22, 2003  
Early View Article  
Published Online June 1, 2004